RNA-dependent synthesis of ergosteryl-3β-O-glycine in Ascomycota expands the diversity of steryl-amino acids

Nathaniel Yakobov[1,§] , Nassira Mahmoudi[1,*,§] , Guillaume Grob[1,‡] , Daisuke Yokokawa[2,‡], Yusuke Saga[2], Tetsuo Kushiro[2], Danielle Worrell[3], Hervé Roy[3], Hubert Schaller[4], Bruno Senger[1] , Laurence Huck[1], Gisela Riera Gascon[1], Hubert D. Becker[1,*], and Frédéric Fischer[1,*]

From the [1]CNRS, Génétique Moléculaire, Génomique, Microbiologie, UMR 7156, Université de Strasbourg, Strasbourg Cedex, France; [2]School of Agriculture, Meiji University, Kawasaki, Kanagawa, Japan; [3]Burnett School of Biomedical Sciences, College of Medicine, University of Central Florida, Orlando, Florida, USA; [4]Plant Isoprenoid Biology (PIB) Team, Institut de Biologie Moléculaire des Plantes du CNRS, Université de Strasbourg, Strasbourg, France

Edited by Karin Musier-Forsyth

A wide range of bacteria possess virulence factors such as aminoacyl-tRNA transferases (ATTs) that are capable of rerouting aminoacyl-transfer RNAs away from protein synthesis to conjugate amino acids onto glycerolipids. We recently showed that, although these pathways were thought to be restricted to bacteria, higher fungi also possess ergosteryl-3β-O-L-aspartate synthases (ErdSs), which transfer the L-Asp moiety of aspartyl-tRNA^{Asp} onto the 3β-OH group of ergosterol (Erg), yielding ergosteryl-3β-O-L-aspartate (Erg-Asp). Here, we report the discovery, in fungi, of a second type of fungal sterol-specific ATTs, namely, ergosteryl-3β-O-glycine (Erg-Gly) synthase (ErgS). ErgS consists of a freestanding DUF2156 domain encoded by a gene distinct from and paralogous to that of ErdS. We show that the enzyme only uses Gly-tRNA^{Gly} produced by an independent glycyl-tRNA synthetase (GlyRS) to transfer glycine onto the 3β-OH of Erg, producing Erg-Gly. Phylogenomics analysis also show that the Erg-Gly synthesis pathway exists only in Ascomycota, including species of biotechnological interest, and more importantly, in human pathogens, such as Aspergillus fumigatus. The discovery of a second type of Erg-aa not only expands the repertoire of this particular class of fungal lipids but suggests that Erg-aa synthases might constitute a genuine subfamily of lipid-modifying ATTs.

Brown and Goldstein stated in 1985 that cholesterol (Cho) "is the most highly decorated small molecule in biology" (https://www.nobelprize.org/prizes/medicine/1985/goldstein/lecture/) (1). Although this statement was meant to describe Cho biosynthesis (2), this can be extended to sterols modifications on the 3β-hydroxyl position, since 3β-O-sulfated (3), acetylated (4), glycosylated (5–7), and fatty acylated sterols (8) have been detected in multiple eukaryotes. Ergosterol (Erg) is one of the most essential lipids found within fungal membranes, whose function mirrors that of Cho in animals (9). Recently, we discovered that numerous species within the Dikarya subkingdom, i.e., higher fungi, such as Aspergillus fumigatus (Afm), Aspergillus oryzae (Aor), and Neurospora crassa (Ncr), produce an aminoacylated sterol that has not been detected in other eukaryotes: ergosteryl-3β-O-L-aspartate (Erg-Asp) (10). It corresponds to Erg onto which aspartic acid (Asp) is esterified on the 3β-hydroxyl through its α-carboxyl (10, 11). Other types of O-acylated sterols found in fungi, such as ergosteryl-acetate (Erg-Ac) (4) or ergosteryl-fatty acids (Erg-FA) (8), are synthesized by acyl-transferases that use acyl-coenzyme A (CoA) as donors of activated acyls (12). Erg-Asp is synthesized by an Erg-Asp synthase, which is a member of the aminoacyl-tRNA transferases (ATTs) family of enzymes (13, 14), that uses aspartyl-transfer RNAs (Asp-tRNA^{Asp}) as a source of activated Asp.

Fungal Erg-Asp synthases (ErdS) (KEGG orthology: K24278) are bifunctional. The N-terminal domain is an aspartyl-tRNA synthetase (AspRS) paralog that, like a regular AspRS (13, 14), uses Asp, ATP, and tRNA^{Asp} to produce Asp-tRNA^{Asp}. The latter is channeled to the C-terminal ATT domain, where Asp is transferred onto the 3β-hydroxyl of Erg, yielding Erg-Asp (10). This domain belongs to the DUF2156 family (or LPG_synthase, PF09924 in the Protein FAMily database (15)), in which other types of ATT are classified (16). For example, aminoacyl-glycerolipid synthases (aaGLSs, with aa denoting the amino acid specificity) are bacterial enzymes that esterify amino acids (aa) in a tRNA-dependent manner onto glycerolipids (GLs) and yield aminoacylated glycerolipids (aaGLs) (17, 18). We also demonstrated that an Erg-Asp hydrolase (ErdH, KEGG orthology: K24279) exists in numerous fungi that removes the Asp moiety of Erg-Asp (10). In bacteria, extracytoplasmic hydrolases of this type deacylate aaGLs and have been shown to exist in gram-positive (19, 20) and gram-negative (21, 22) bacteria.

To date, cellular functions of Erg-Asp in the physiology of Dikarya remain unknown and this compound is the first and single example of a 3β-O-L-aminoacyl derivative of sterols (10).

In contrast, bacterial aaGLSs carrying distinct substrate specificities produce a variety of aaGLSs (23, 24) using various GLs, such as phosphatidylglycerol (PG), cardiolipin, diacylglycerol, as well as various aa-tRNAs (17, 18). Several paralogs of aaPGSs sometimes coexist in bacterial species (20), such as in *Clostridium perfringens*, where a LysPGS and an AlaPGS produce LysPG and AlaPG, respectively, whereas in *Enterococcus* spp., one single aaGLS of broad aa-tRNA specificity (23) synthesizes Ala-, Lys- and ArgPG (24). Given this bacterial diversity, we considered the possibility that Erg-Asp could be one instance of a larger family of aminoacylated sterols in fungi.

Here we report the discovery in Ascomycota, one of the two divisions of Dikarya, of a novel type of DUF2156 proteins. They are all free-standing DUF2156 domains (fDUF2156) phylogenetically related and paralogous to ErdS that, contrary to the latter, are not fused to an aminoacyl-tRNA synthetase (aaRS). Using *Afm*, *Aor*, and *Yarrowia lipolytica* (*Yli*) as models, we demonstrate that fungal fDUF2156 proteins have an enzymatic activity distinct from that of ErdS: they reroute glycyl-tRNA^{Gly} (Gly-tRNA^{Gly}) produced by a glycyl-tRNA synthetase (GlyRS) and transfer Gly onto the 3β-hydroxyl of Erg, yielding ergosteryl-3β-*O*-glycine (Erg-Gly), another and previously undetected type of sterol conjugate of the 3β-*O*-aminoacyl-type. We therefore name those enzymes Erg-Gly synthases (ErgS, Er: ergosterol, g: glycine, S: synthase). ErgSs expand the repertoire of the newly discovered class of ergosteryl-amino acid synthases. We conclude that ErgS and ErdS represent two members of a new subfamily of AATs, namely, tRNA-dependent ergosteryl-3β-*O*-amino acid synthases, or ErxS (x denoting one of the 20 canonical protein amino acids).

Results

A second type of DUF2156 proteins in Ascomycota

After the discovery of ErdS in Dikarya (10), we noticed that *Afm* and *Aor* possess an additional protein that presents distant homology (∼20% identity) to the ATT domain of ErdS and that is recognized as a DUF2156 protein by the PFAM search tool (15). Both proteins, encoded by the AFUA_8g01260 and AO090011000521 genes in *Afm* and *Aor*, respectively, are free-standing DUF2156 domains (fDUF2156, from now on shortened fDUF), meaning that they are fused neither to an aaRS domain nor to an N-terminal integral membrane aaGLSs flippase domain, unlike fungal ErdS (10) or bacterial MprFs (17), respectively (Fig. 1, *A* and *B*). Sequence searches revealed that fDUF proteins were also present in *Beauveria bassiana* (*Bba*, Sordariomycetes, gene: BBA_06338 in the ARSEF 2860 strain) and *Y. lipolytica* (*Yli*, Saccharomycetes, gene: YALI0E00330g). Sequence analyses and structure predictions of *Afm*, *Bba*, and *Yli* fDUFs (Fig. S1) show that, like for the ATT domain of ErdS (10) or bacterial aaGLSs, these proteins are all likely constituted of two Gcn5-like *N*-acetyltransferase (GNAT) domains separated by a positively charged α helix (α$^{(+)}$ helix), a fold characteristic of ATTs of the DUF2156 family (17, 25, 26) (Figs. 1*A* and S1). Depending on their host organism, fDUF proteins have N-terminal extensions of varying sizes (Fig. 1*B*) that share neither homology to known proteins nor obvious subcellular localization signals (PSORT II, https://psort.hgc.jp/form2.html). In the case of *Aor*, however, the fDUF2156 protein seems much shorter than its closest homologs in *Afm* or in *Aspergillus flavus* (*Afv*), with which it shares close ancestry (27, 28). The GNAT II domain appears dramatically truncated (Fig. S1), to the point that most of the putative ATT active site would be absent, suggesting that the enzyme would very likely be inactive (Fig. 1*B* and see below).

Because fDUF proteins are not fused to an aaRS, and because the substrate specificities of DUF2156 proteins cannot be predicted based on consensus sequences (17), *in silico* determination of the aa-tRNA or acceptor lipid substrates were impossible. However, phylogenetic reconstructions (Fig. 1*C*) showed that fungal ErdS and fDUF are related to the DUF2156 domains of bacterial aaGLSs (MprFs). The latter are known to produce only
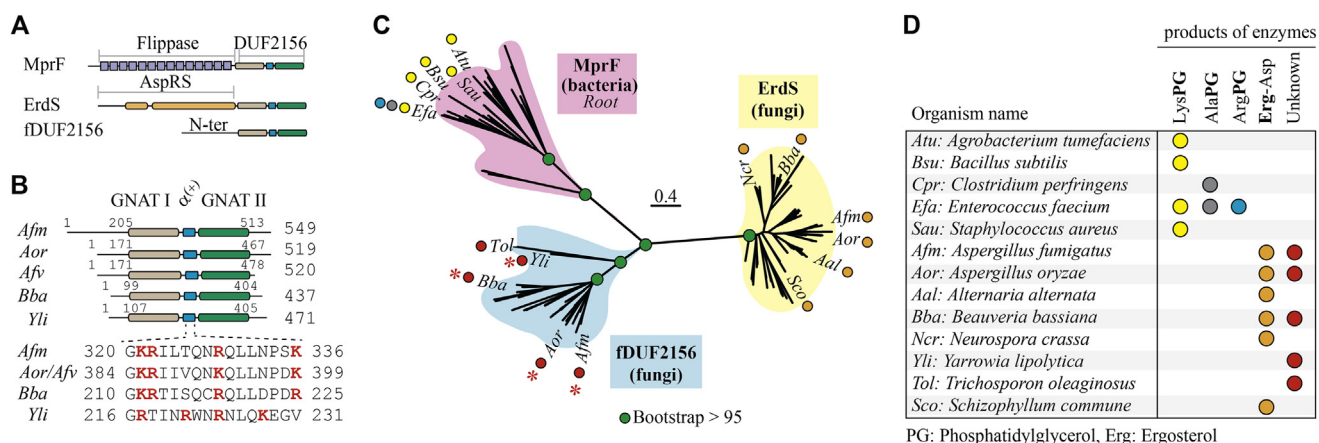

Figure 1. *In silico* characterization of fungal fDUF2156 proteins. *A*, architecture of bacterial aaGLSs (MprFs), with the N-terminal aaGLs flippase (14 transmembrane helices) and the DUF2156 domain. Fungal ErdS (AspRS-DUF2156) are represented as well as fungal fDUF2156 proteins. *B*, fDUF proteins from *Afm*, *Aor*, *Afv*, *Bba*, and *Yli*. The two Gcn5-N-acetyltransferase (GNAT) domains separated by the α$^{(+)}$ helix, which constitute the DUF2156 fold, are detailed (domain coordinates indicated, length of proteins on the *right*). K (Lys) and R (Arg) residues are shown in *red*. *C*, maximum likelihood phylogenetic reconstruction of bacterial (MprF) and fungal (ErdS, fDUF) DUF2156 domains. Three clades are visible that match bacterial MprF- (*purple background*), ErdS- (*yellow background*), and fDUF2156- (*blue background*) specific groups. Positions of some proteins are indicated with the abbreviated name of the organism in which they are found together with (*D*) the aminoacylated products that they synthesize (if known). *Red asterisks* indicate the proteins studied in this work.

aaGLs (Fig. 1*D*) (17, 20), whereas all ErdSs tested yield Erg-Asp (10), making these lipid modifications clade specific. Of interest, ErdS and fDUFs form two distinct and robust clades (Fig. 1*C*), related to aaGLSs, suggesting that they might represent two types of enzymes, possibly with different activities and/or specificities. ErdS and fDUFs coexist in *Afm*, *Aor*, *Bba*, and many other Ascomycota (Fig. 1*D* and see below), which reinforces the idea that they might have different and nonredundant activities and/or specificities, like paralogous aaPGSs in bacteria (17, 18). These evolutionary relationships of fDUFs with either ErdSs or aaGLSs, as well as their structural features, supported the hypothesis that they could modify lipids—glycerolipids or Erg—by a tRNA-dependent mechanism similar to that of ErdS (10, 17). We therefore inferred that fDUFs might be able to bind an aa-tRNA of unknown identity and produced by an unknown aaRS to use it for the tRNA-dependent modification of an unknown lipid.

Freestanding DUF2156 proteins modify lipids

In order to determine whether fDUF proteins are involved in the tRNA-dependent aminoacylation of a lipid, we tried to construct Δ*fDUF* mutants in *Afm* to be able to identify the lipid species that would disappear in total lipids from deletion strains, when analyzed by thin layer chromatography (TLC) compared with the WT lipid content. Despite multiple attempts in *Afm* using electroporation (10, 29) to introduce the deletion cassette, we failed to isolate Δ*fDUF* mutants. However, our *in silico* analyses show that the yeast *Saccharomyces cerevisiae* (*Sce*) lacks not only ErdS (10) but also fDUF proteins (see below). The use of *Sce* previously greatly facilitated the identification of Erg-Asp through heterologous expression of ErdS, followed by TLC lipid profiling (10). We therefore applied the

same strategy to fDUF proteins from diverse representative species within the fDUF clade (*Afm*, *Aor*, *Bba*, and *Yli*) (Fig. 1*C*). Genes from *Afm*, *Bba*, and *Yli* presented no introns, so they were PCR-amplified from genomic DNA and cloned into expression vectors for *Sce*. In the case of *Aor*, the shortest form described above (Fig. 1*B* and S1) was unexpected. Closer examination of sequences showed that this was an artifact likely originating from misannotation of an intron (see Fig. S2 and Supporting Methods for details). We amplified the longest form that was used for heterologous expression in *Sce*.

We first extracted total lipids from WT and *Afm* fDUF-expressing *Sce* strains (*Sce*+*Afm* fDUF) and separated them by TLC, using a solvent system that was appropriate to visualize Erg-Asp (10), *i.e.*, $CHCl_3$:CH_3OH:H_2O (130:50:8, v:v:v). Comparison of lipid profiles from the two strains revealed that a novel lipid termed lipid Y (LY) and absent from the WT strain (*Sce*) was produced by the *Sce*+*Afm* fDUF strain (Fig. 2*A*). LY displayed different migration properties than the Erg-Asp produced by *Afm* ErdS (*Sce*+*Afm* ErdS), denoting that the two enzymes have distinct enzymatic activities and synthesize distinct products. LY migrated close to the solvent front, indicating that it was more hydrophobic than Erg-Asp. Like Erg-Asp, it stained with a distinctive brownish color with a $MnCl_2$/H_2SO_4 solution (30), suggesting that it could also be an Erg or sterol derivative (Fig. 2*A*) (10). LY weakly but positively stained with ninhydrin and was degraded under alkaline conditions (Fig. S3), which supported the hypothesis that it was likely an aminoacylated sterol in which the amino acid and sterol are linked by an ester (alkaline-sensitive) bond, like in Erg-Asp (10). In order to better visualize LY on TLC, we used the $CHCl_3$:CH_3OH:H_2O (130:16:1, v:v:v) mobile phase (Fig. 2*B*). Under these better resolving conditions, we
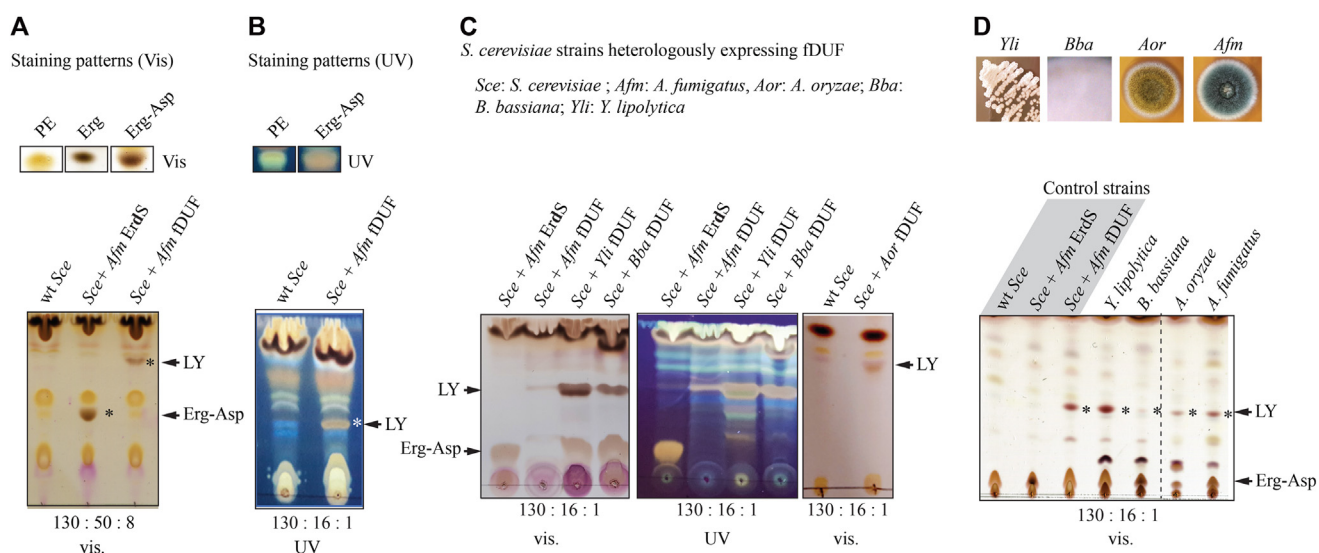

Figure 2. Ascomycetes possess an fDUF, whose heterologous expression in *S. cerevisiae* triggers production of a novel lipid. *A*, heterologous expression of *Afm* ErdS (*Sce*+*Afm* ErdS) and fDUF in *Sce* (*Sce*+*Afm* fDUF). Total lipids were separated with the $CHCl_3$:CH_3OH:H_2O (130:50:8, v:v:v) solvent, stained with $MnCl_2$/H_2SO_4 and visualized under white (vis.) light. Control lipid bands (*upper panel*) were used to illustrate the staining of sterols under visible or UV light. Asterisks indicate Erg-Asp and LY bands. *B*, TLC analysis of total lipids extracted from a wt and *Afm* fDUF *Sce*-expressing strains with the $CHCl_3$:CH_3OH:H_2O (130:16:1, v:v:v) solvent. TLC was visualized under UV light. *C*, TLC analysis of total lipids extracted from *Sce* strains expressing the indicated proteins: *Sce*+ *Afm* ErdS (Erg-Asp production), and *Sce*+ *Afm*-, or *Bba*-, or *Yli*-, or *Aor* fDUF (LY production). *D*, separation on HPTLC plates of total lipids from the indicated fungal strains (illustrated in the *upper panel*) compared with control strains: *Sce* WT, *Sce* + *Afm* ErdS, and *Sce* + *Afm* fDUF; the $CHCl_3$:CH_3OH:H_2O ratios (v:v:v) are indicated. Erg, ergosterol; LY, lipid Y; PE, phosphatidylethanolamine.

visualized that *Afm*, *Aor*, *Bba*, and *Yli* fDUF proteins led to the production of the exact same LY when expressed in *Sce*, e.g., shared the same migration and staining properties (Fig. 2*C*). Finally, we analyzed total lipid extracts from WT strains of *Afm*, *Aor*, *Bba*, and *Yli* and confirmed in each case that a lipid band with similar migration and staining properties as LY was present (Fig. 2*D*), with the exception of *Bba*, which, under the growth conditions used, produced only barely detectable levels of LY. In conclusion, upon heterologous expression in *Sce*, all tested fDUFs produce the same LY with identical migration and staining properties. This identical LY is also naturally present in *Afm*, *Aor*, *Bba*, and *Yli*, regardless of their positions within the fDUF-specific clade (Fig. 1*D*).

fDUF2156 proteins produce an ergosteryl-3β-O-amino acid

We next used total lipids from *Yli* that naturally expresses fDUF and produces the highest yields of LY (Figs. 1*C* and 2) and purified LY using flash column chromatography (FC) (Figs. 3*A* and S3) (10, 20). LC-MS^n analyses of the resulting fractions revealed the presence of protonated ions of dehydrated ergosterol ([Erg-H$_2$O + H]$^+$, m/z = 379, see (10)), as well as of a compound at an m/z of 907. MS^n analysis of this latter compound revealed a fragmented ergosterol ion at m/z = 379, suggesting that the parent ion (m/z = 907) maybe a protonated dimeric ion of glycylated ergosterol ([2ErgGly+H]$^+$, m/z = 907), which would imply that LY would be, like Erg-Asp, an aminoacylated sterol, most likely an ergosteryl-3β-O-
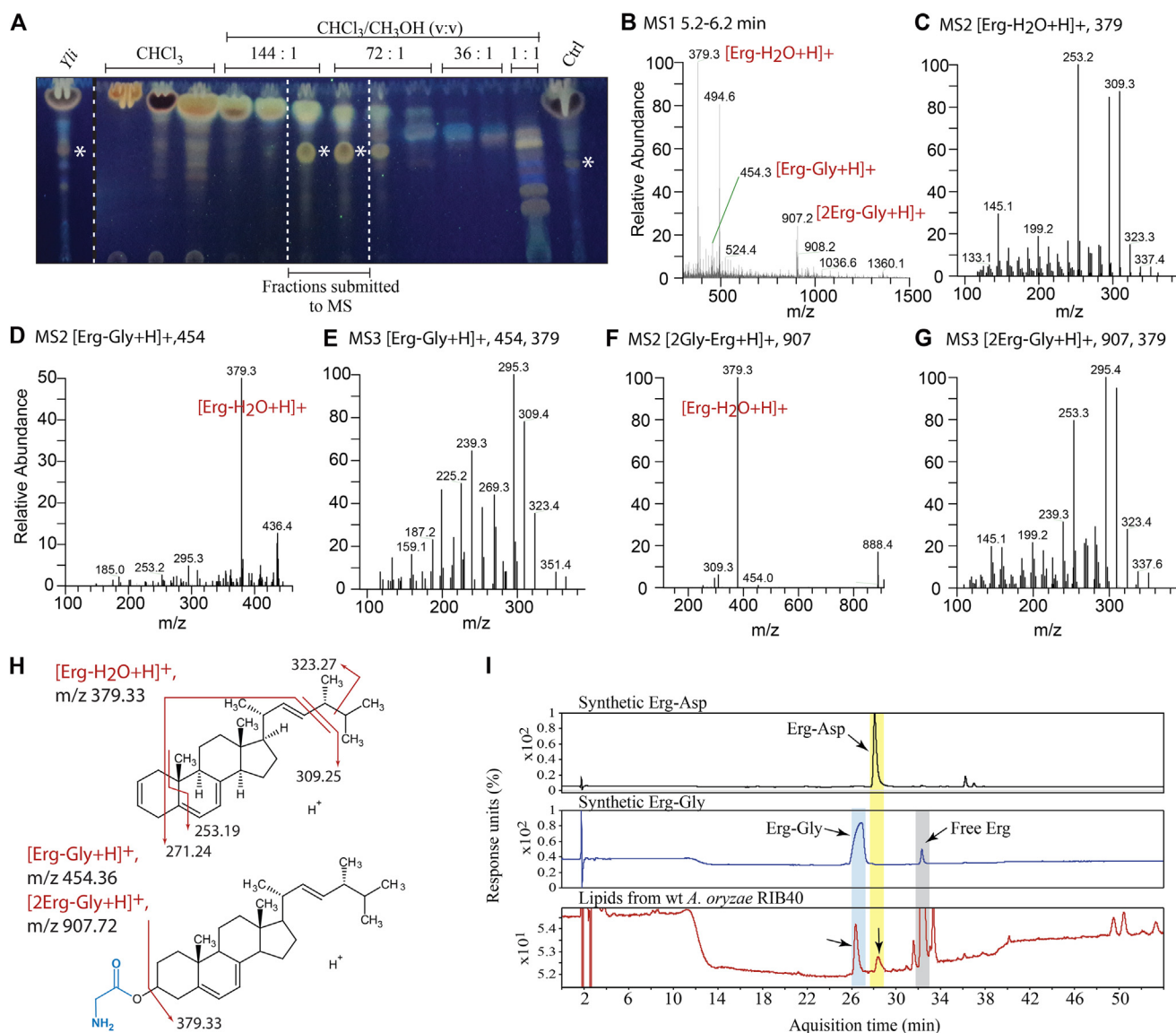

Figure 3. Purification and LC-MS^n analysis of LY from *Y. lipolytica* and characterization of LY in *A. oryzae*. *A*, LY was purified from *Yli* total lipids by flash chromatography on silica gel 60 column. The TLC shows fractions from the purification. Apolar lipids eluted with CHCl$_3$ and LY with CHCl$_3$:CH$_3$OH (v:v) solvents of increasing polarity. *Yli*, total lipids; Ctrl, total lipids from the *Sce*+ *Yli* fDUF strain. *Asterisks* indicate LY. *B*, MS1 spectrum between 5.2 to 6.2 min, (*C*) MS2 spectrum of ergosterol [Erg-H$_2$O + H]$^+$ at m/z = 379, (*D*) MS2 spectrum of ergosteryl-3β-O-glycine (Erg-Gly) [Erg-Gly+H]$^+$ at m/z = 454, and (*E*) its MS3 spectrum at m/z = 379 (454→379). *F*, MS2 spectrum of the ion complex Erg-Gly [2Gly-Erg+H]$^+$ at m/z = 907, and (*G*) its MS3 spectrum at m/z = 379 (907→379). *H*, structure of the ions of ergosterol [Erg-H$_2$O + H]$^+$, Erg-Gly [Erg-Gly+H]$^+$ and MS2 fragmentations. MS^n data are shown for peaks annotated in *red*. MS2 fragmentation of ergosterol is identical to that previously described (e.g., (10)). *I*, HPLC separation of total lipids extracted from wt *Aor* RIB40 that naturally expresses both ErdS and ErgS. Eluted compounds were monitored at 282 nm and peaks of interest were submitted to an Accurate-Mass Q-TOF LC-MS to confirm their identity. Synthetic Erg-Gly and Erg-Asp were used as a standard to identify, in total lipids, Erg-Gly and Erg-Asp.

glycine (Erg-Gly), at least in *Yli* (Fig. 3). To test this hypothesis, we prepared (11) synthetic Erg-Gly ($_{syn}$Erg-Gly) and analyzed it by the same methods. $_{syn}$Erg-Gly and an FC-purified fraction both exhibited a peak at m/z = 907 and identical fragmented ion products upon MS^n analysis. Tuning the instrument to the m/z peak at 907 using $_{syn}$Erg-Gly allowed detection of the monomeric protonated ion [ErgGly+H]$^+$ at m/z = 454 both in the synthetic Erg-Gly preparation and in the FC-purified sample (Figs. 3 and S4).

To test whether other fDUF protein candidates also synthesize Erg-Gly, LC-MS^n analyses were carried out on total lipid extracts originating from the *Sce+ Afm* fDUF strain, alongside the wt *Sce* strain (Figs. S3 and S4). Erg-Gly was detected in the dimeric ion form ([2GlyErg+H]$^+$, m/z = 907) in the lipids extracted from the *Sce+ Afm* fDUF strain but was absent from wt lipids (Fig. S4). Similarly, HPLC separation of total lipids from the *Sce+ Aor* fDUF strain showed that an additional lipid identical to $_{syn}$Erg-Gly, absent from a wt or an empty plasmid-carrying strain, could be detected (Fig. S5). Finally, we analyzed total lipids extracted from wt *Aor* RIB40 by HPLC. Comparison of profiles with standard profiles obtained with the synthetic Erg-Gly and Erg-Asp that we prepared (11) confirmed that Erg-Gly was present, together with Erg-Asp (Fig. 3*I*), in agreement with the fact that this fungus possesses a functional ErdS (10) and fDUF (Fig. 1 and see below).

In conclusion, Erg-Gly could be formally detected not only in *Yli* and *Aor* total lipids but also in total lipids extracted from *Sce* strains heterologously expressing *Afm* and *Aor* fDUF, demonstrating that the three enzymes (from *Afm*, *Aor*, and *Yli*) produce the same aminoacylated sterol *in situ* (in *Aor* and *Yli*) as well as when heterologously expressed (in *Sce*). *Bba* fDUF,

although not characterized by MS, produces the same aminoacylated lipid, since its properties on TLC (Fig. 2, *C* and *D*) are equivalent to those of Erg-Gly produced by *Afm*, *Aor*, and *Yli* enzymes. Therefore, because fDUF is a homolog of ErdS (Fig. 1), all these results advocate for the hypothesis that fDUF proteins aminoacylate Erg using Gly-tRNA^{Gly} as a Gly donor, making them putative ergosteryl-3β-*O*-glycine synthases, or ErgS (Er: ergosterol, g: glycine, S: synthase).

Mutations in the α$^{(+)}$ helix suggest that ErgS is aa-tRNA dependent *in vivo*

Erg aspartylation by ErdS (10) and addition of Lys, Arg, or Ala onto glycerolipids by aaGLSs (17) are all strictly aa-tRNA dependent. This is also the case for other transferases that modify other types of macromolecules (16, 31). In the case of aaPGSs, the α$^{(+)}$ helix found between GNAT domains I (lipid binding) and II (aa-tRNA binding) (Fig. 1) is crucial to the aa-tRNA substrate utilization, likely because this positively charged helix helps binding the tRNA acceptor arm through charge interaction with the ribose-phosphate backbone of tRNA (26). In the case of ErgS, utilization of Gly-tRNA^{Gly} was expected (Fig. 3). In order to verify the tRNA dependency of the reaction, we first used an *in vivo* approach and heterologously expressed in *Sce* either wt *Afm* ErgS or variants of the enzyme mutated in the α$^{(+)}$ helix (Fig. 1*B*) in order to determine whether mutations impaired Erg-Gly synthesis. K321, R322, R328, and K336 were mutated into glutamate residues in three different combinations (Fig. 4*A*), yielding helices with negatively charged side chains that, according to the tRNA binding hypothesis, should repel tRNA and decrease Erg-Gly accumulation. *Afm* ErgSα$^{(+/-)}$, in which K321 and R322 were mutated to E (R328 and K335 remained unchanged), ErgS

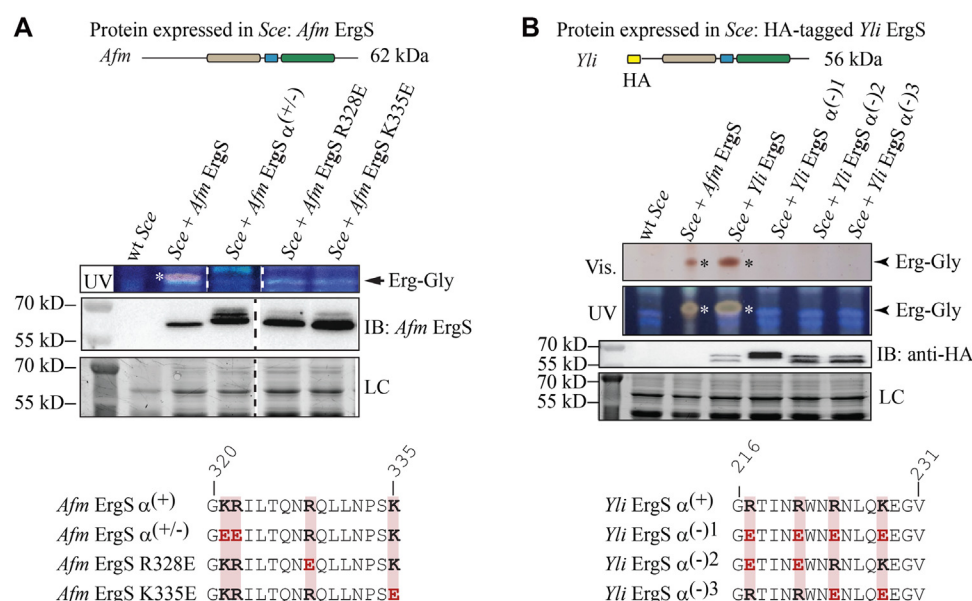**Figure 4. Mutation of the α$^{(+)}$ helix suggests that Erg-Gly synthesis is tRNA dependent *in vivo*.** *A*, *Afm* ErgS and three mutants of the α$^{(+)}$ helix (described at the *bottom*) or (*B*) *Yli* HA-tagged ErgS and three mutants of the α$^{(+)}$ helix (described at the *bottom*) were expressed in *Sce*. TLCs were developed in the CHCl$_3$:CH$_3$OH:H$_2$O (130:16:1, v:v:v) solvent, stained with MnCl$_2$/H$_2$SO$_4$ and visualized under white (vis.) or UV light. *Asterisks* indicate the position of Erg-Gly. Immunoblots were also performed on whole extracts to detect expression of *Afm* ErgS (and mutants) using anti-*Afm* ErgS antibodies, or anti-HA antibodies to detect *Yli* HA-ErgS (and mutants). LC, loading control (strain free).

R328E, and ErgS K335E (in which only one residue at a time was mutated) were used (Fig. 4*A*). Results showed that, as hypothesized, wt *Afm* ErgS produces Erg-Gly in *Sce*, whereas all three mutants failed to synthesize detectable amounts of the Erg-Gly. Anti-*Afm* ErgS antibodies were used to confirm that the enzyme was expressed in all cases. Note that, when expressed in *Sce* and analyzed by Western blot, bands of *Afm* ErgS mutants, but not of the wt enzyme, appear as doublets, which likely accounts for putative mobility changes due to the mutations introduced or possible posttranslational modifications.

As already observed, Erg-Gly levels were very low in the *Sce+Afm* fDUF (ErgS) strain, when compared with those of the *Sce+Yli* fDUF strain (Fig. 2*C*). We therefore generated *Sce* strains expressing three *Yli* fDUF variants mutated in the $\alpha^{(+)}$ helix (residues 216–231) (Fig. 4*B*).We named these mutants *Yli* ErgS $\alpha^{(-)1}$ when R217, R221, R224, and K228 were all mutated to E; *Yli* ErgS $\alpha^{(-)2}$ when R217 and R221 were mutated to E; and *Yli* ErgS $\alpha^{(-)3}$, when mutation of R224 and K228 to E were present (Fig. 4*B*). Similar to *Afm* ErgS, all *Yli* ErgS mutants were defective in Erg-Gly synthesis, which again supported the hypothesis that the $\alpha^{(+)}$ helix is essential. Since our anti-*Afm* ErgS antibodies did not cross-react with *Yli* ErgS (Fig. S6), we expressed the wt and mutant *Yli* enzymes as N-terminally HA-tagged versions. In all cases, the enzymes were expressed, but no Erg-Gly synthesis was detected for the HA-tagged mutant versions, in contrast to the HA-tagged wt enzyme. Taken together, and given the role attributed to the $\alpha^{(+)}$ helix (26), our results strongly support that *Afm* and *Yli* ErgS are, as hypothesized, aa-tRNA dependent and, more specifically, Gly-tRNA^{Gly} dependent, a hypothesis that we decided to analyze in more detail *in vitro*.

Erg-Gly synthesis strictly depends on Gly-tRNAs

Erg-Gly, like Erg-Asp, is a 3β-*O*-ester of sterol and formation of ester bonds is nonspontaneous under physiological conditions (32), implying that ErgS must use an activated form of Gly. As for all similar ATTs (10, 31), it must be an aa-tRNA, here Gly-tRNA^{Gly}. Gly-tRNA^{Gly} is produced by GlyRS, reason for which we expressed and purified recombinant *Yli* His$_6$-GlyRS. GlyRS sequentially produces two forms of activated Gly: glycyl-adenylate (Gly~AMP) and Gly-tRNA^{Gly} itself (Fig. 5*A*) that could be utilized by ErgS. In order to decipher Erg glycylation by ErgS *in vitro* and to understand each step of the reaction (Fig. 5*A*), we expressed *Afm* and *Yli* ErgS in *Escherichia coli* as maltose-binding protein (MBP) fusions to improve solubility of the recombinant enzymes and purified them by affinity chromatography. With those enzymes, we performed a series of experiments in order to determine which of the GlyRS products was used by ErgS.

In Figure 5*A*, we present the overall reactions catalyzed by GlyRS and ErgS and, below, the different steps to which re-actions can proceed under the various experimental conditions that we tested to understand which substrates were required for activity. In the presence of [^{14}C]Gly, ATP, and either total tRNA or partially fractionated tRNA^{Gly}, *Yli* His$_6$-GlyRS synthesized [^{14}C]Gly-tRNA^{Gly} (Fig. S7). [^{14}C]Gly-tRNA^{Gly} could

also be produced using GlyRS from wt *Sce* crude protein extract (Fig. 5*B*, left panel). [^{14}C]Gly-tRNA^{Gly} plateau typically reached ~60 pmol per reaction. Adding *Yli* MBP-ErgS to a mixture containing *Yli* His$_6$-GlyRS, partially fractionated *Sce* tRNA^{Gly}, ATP, [^{14}C]Gly, and Erg confirmed that a radiolabeled band (Fig. 5*B*, right panel, lane 3) with migration properties similar to our $_{syn}$Erg-Gly (10, 11) (Fig. 5*B*, middle panel) was observed, which we therefore attributed to Erg-[^{14}C]Gly. In parallel, we used purified *Afm* ErdS (10), in the presence of [^{14}C]Asp, pure *Sce* tRNA^{Asp}, ATP, and Erg and verified that it produced Erg-[^{14}C]Asp (Fig. 5*B*, right panel, lane 1), which had very distinct migration properties as compared with Erg-[^{14}C]Gly under the same TLC conditions. None of the enzymes was active when RNase A, which degrades tRNAs, was added. This confirmed the tRNA dependency of the reaction. Since Erg-Gly synthesis occurred *in vitro*, we further investigated ErgS activity. For yet unknown reasons, purified recombinant *Afm* MBP-ErgS was inactive *in vitro*, suggesting that it lost its activity upon purification from *E. coli* or that the MBP tag hindered activity (Fig. S7 and see below). Furthermore, Erg-Gly accumulation *in vivo* in the *Sce+Afm* ErgS strain was also much lower than in the *Sce+Yli* ErgS strain (Fig. 2*C*), which prompted us to focus on recombinant *Yli* MBP-ErgS for further *in vitro* investigations.

TLC analyses of reaction products under various conditions (Fig. 5, *A* and *C*) revealed that, upon [^{14}C]Gly-tRNA production, addition of *Yli* MBP-ErgS enabled the synthesis of Erg-[^{14}C]Gly when either pure Erg or total lipids from *Sce* (containing Erg) were used as acceptors (Fig. 5*C*, lanes 1 and 6). In contrast, the *Yli* MBP-ErgS$\alpha^{(-)1}$ mutant (described in Fig. 4*B*) was inactive (Fig. 5*C*, lane 2), thereby confirming the essentiality of the $\alpha^{(+)}$ helix for activity. As expected, in the absence of ErgS (Fig. 5*C*, lane 3), total lipids, or Erg (Fig. 5*C*, lane 4), no Erg-[^{14}C]Gly could be detected, meaning that the reaction depended on the presence of ErgS and on Erg, either pure or in total lipids. As already described above, addition of RNase A (Fig. 5*C*, lanes 5 and 7) resulted in the absence of Erg-[^{14}C]Gly production. In agreement, when *Yli* His$_6$-GlyRS was present, but tRNA absent (Fig. 5*C*, lane 9), *Yli* MBP-ErgS could not use glycyl-adenylate (Gly~AMP) produced under these conditions by GlyRS to synthesize Erg-[^{14}C]Gly. This confirmed that ErgS uses only Gly-tRNA and not Gly~AMP as a source of activated Gly. In the absence of GlyRS (Fig. 5*C*, lane 8), ErgS was, as expected, not able to synthesize Erg-[^{14}C]Gly, demonstrating that free and nonactivated Gly is not a substrate of ErgS. Note that, sometimes, Erg-[^{14}C]Gly or Erg-[^{14}C]Asp bands may appear as doublets, which denotes the fact that Erg may be oxidized, yielding an aspartylated oxidized sterol with slightly different migration properties than Erg-Gly or Erg-Asp, respectively.

In line with ErgS's specificity for Gly-tRNA^{Gly}, when *Yli* MBP-ErgS was added to a reaction mixture containing only Erg and no GlyRS, ATP, free tRNA, or free [^{14}C]Gly, *i.e.*, making [^{14}C]Gly-tRNA^{Gly} synthesis impossible, Erg-[^{14}C]Gly synthesis could be initiated only with addition of preformed [^{14}C]Gly-tRNA^{Gly} (~200 nM), unless RNase A was added (Fig. 5*D*). When increasing concentrations of cold
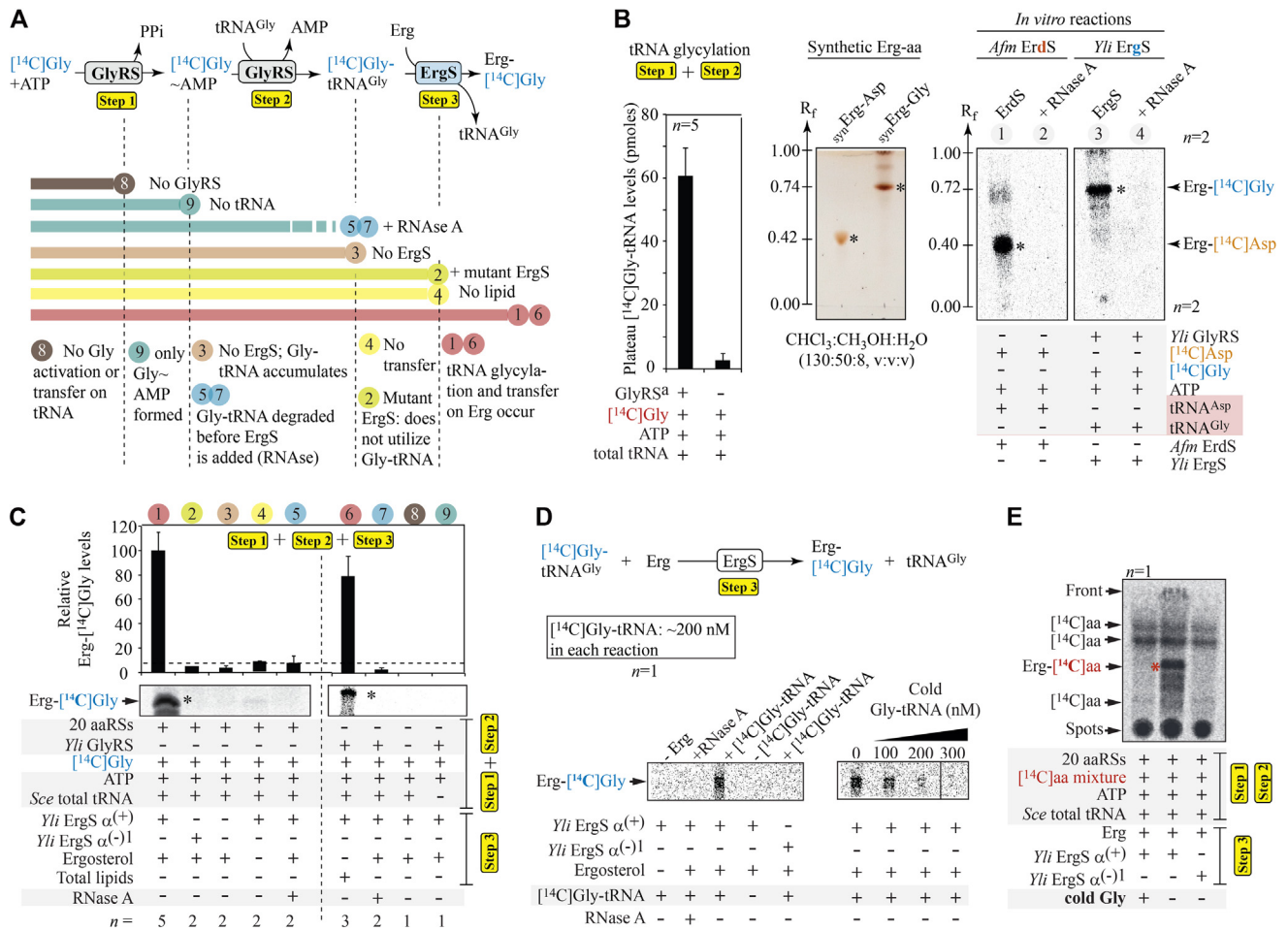
Figure 5. *In vitro* investigation of Erg-Gly synthesis by ErgS. *A*, Erg-Gly synthesis reaction scheme (coupled reaction, when GlyRS and ErgS are present at the same time). *Step 1*: Gly activation into Gly∼AMP by GlyRS and *step 2*: transfer onto tRNA^{Gly}; *step 3*: Erg-Gly synthesis from Gly-tRNA^{Gly}. Colored bands below the scheme indicate up to which step the coupled reaction proceeds, when the indicated component (*right side*) is omitted (−) or added (+). Numbers refer to the lanes presenting the *in vitro* results in (*C*). *B, left panel*, [^{14}C]Gly-tRNA^{Gly} synthesis by *Yli*His$_6$-GlyRS or total aaRS extracts (containing GlyRS) from wt *Sce* in a typical coupled reaction. Results are identical for both sources of GlyRS (denoted by GlyRS^a). *Middle panel*, control TLC showing mobility of synthetic Erg-Asp and Erg-Gly in the CHCl$_3$:CH$_3$OH:H$_2$O (130:50:8, v:v:v) mobile phase. *Right panel*, control reactions with purified *Afm* ErdS (produces Erg-[^{14}C]Asp, indicated with an *asterisk*, and a second band (**) discussed below) and purified *Yli* MBP-ErgS with the indicated components. ErgS produces a compound (*) with properties identical to $_{syn}$Erg-Gly, showing that it synthesizes Erg-Gly. *C*, Erg-[^{14}C]Gly synthesis experiments under the indicated conditions (+, presence; −, absence of the indicated components). *Yli* MBP-ErgS (or mutated ErgS) was added to [^{14}C]Gly-tRNA^{Gly} produced by *Sce* GlyRS (in a total protein extract) or *Yli*His$_6$-GlyRS in the presence/absence of various substrates and/or RNase A. Asterisks indicate position of Erg-[^{14}C]Gly. *D*, Erg-[^{14}C]Gly synthesis (step 3 only) with added [^{14}C]Gly-tRNA (∼200 nM) and increasing amounts of cold Gly-tRNA (100–300 nM). *E*, isotopic competition of cold Gly for Erg-[^{14}C]Gly synthesis. 15 [^{14}C]aa-tRNAs were synthesized with 15 aaRSs (*Sce* total proteins), from 15 [^{14}C]aa and total *Sce* tRNA, to which Erg, ErgS, the ErgSα$^{(-)1}$ mutant, or RNase A was added. [^{14}C]aa indicate bands attributed to free radiolabeled amino acids present in the reaction and separated by TLC. The *red asterisk* indicates Erg-[^{14}C]Gly. In all cases, bars indicate standard deviation and the number of replicates is indicated.

Gly-tRNA^{Gly} (100–300 nM) were used to compete free [^{14}C]Gly-tRNA^{Gly}, the intensity of Erg-[^{14}C]Gly bands correlatively decreased on TLC, indicating strong and specific isotopic competition (Fig. 5D). In parallel, to probe ErgS's aa-tRNA specificity, we used a *Sce* total protein extract, containing all aaRSs, a mix containing 15 [^{14}C]aa (lacking Asn, Gln, Cys, Met, and Trp), total *Sce* tRNA, and ATP to produce the 15 corresponding [^{14}C]aa-tRNAs (∼50,000 cpm per reaction when plateaus were reached, Fig. S7). To these 15 [^{14}C]aa-tRNAs, we added *Yli* MBP-ErgS and observed that a band corresponding to Erg-[^{14}C]Gly was present, which completely disappeared on TLC when excess unlabeled cold Gly was added (Fig. 5E), showing that, of the 15 [^{14}C]aa used, only Gly-tRNA^{Gly}, formed by GlyRS, is used by ErgS. Again, no Erg-[^{14}C]Gly was observed when the *Yli* MBP-ErgS α$^{(-)1}$ mutant was used.

Specificity of ErgS and ErdS

ErdS produces its own Asp-tRNA^{Asp} from ATP, Asp, and tRNA^{Asp}, and the *cis*-acting transferase (DUF2156) domain uses it to transfer Asp onto Erg. In contrast, ErgS uses a Gly-tRNA^{Gly} substrate produced in *trans* by an independent GlyRS (Figs. 5 and 6A). Because ErdS and ErgS are homologous (Fig. 1B), we wondered whether these enzymes could or not display functional promiscuity both *in vitro* and *in vivo*. ErgS is not expected to use Asp-tRNA^{Asp} (Fig. 6A). We first verified it *in vivo* using *Sce* strains (Fig. 6B) expressing ErdS alone (*Sce*+*Afm* ErdS), ErgS alone (*Sce*+*Afm* ErgS), or both enzymes at the same time (*Sce*+*Afm* ErdS+*Afm* ErgS). Heterologous expression was confirmed by Western blot (Fig. 6C, upper panel and Fig. S8) using anti-*Afm* ErdS and anti-*Afm* ErgS antibodies, before extracting total lipids to analyze them by TLC. An *Sce* strain expressing an ErdS version deleted from its

Erg-Asp synthase/DUF2156 domain (ErdSΔDUF) was used as a negative control. Results show that only Erg-Asp accumulates when ErdS is expressed, with no detectable Erg-Gly. In contrast, Erg-Gly is detected when ErgS is expressed, with no Erg-Asp visible on TLC. Coexpression of ErdS (in the form of ErdS-GFP fusion) and ErgS resulted in the accumulation of both Erg-Asp and Erg-Gly.

In parallel, we tested Erg-[14C]Asp and Erg-[14C]Gly synthesis activities in protein extracts from all strains *in vitro*

(Figs. 6C and S8). To this end, we extracted total proteins from each strain and separated soluble (S100) and membrane-bound proteins (P100) by centrifugation. As expected, we detected Erg-[14C]Asp synthesis in total, S100, and P100 extracts from the *Sce+Afm* ErdS (Fig. 6C, lower panel, lanes 4–6) and *Sce+Afm* ErdS+*Afm* ErgS (lanes 10–12) strains, while Erg-[14C]Gly only occurred in *Sce+Afm* ErgS (lanes 7–9) and *Sce+Afm* ErdS+*Afm* ErgS strains (lanes 10–12). No activity was detected in the control *Sce* strain (lanes 1–3). Activity of ErdS
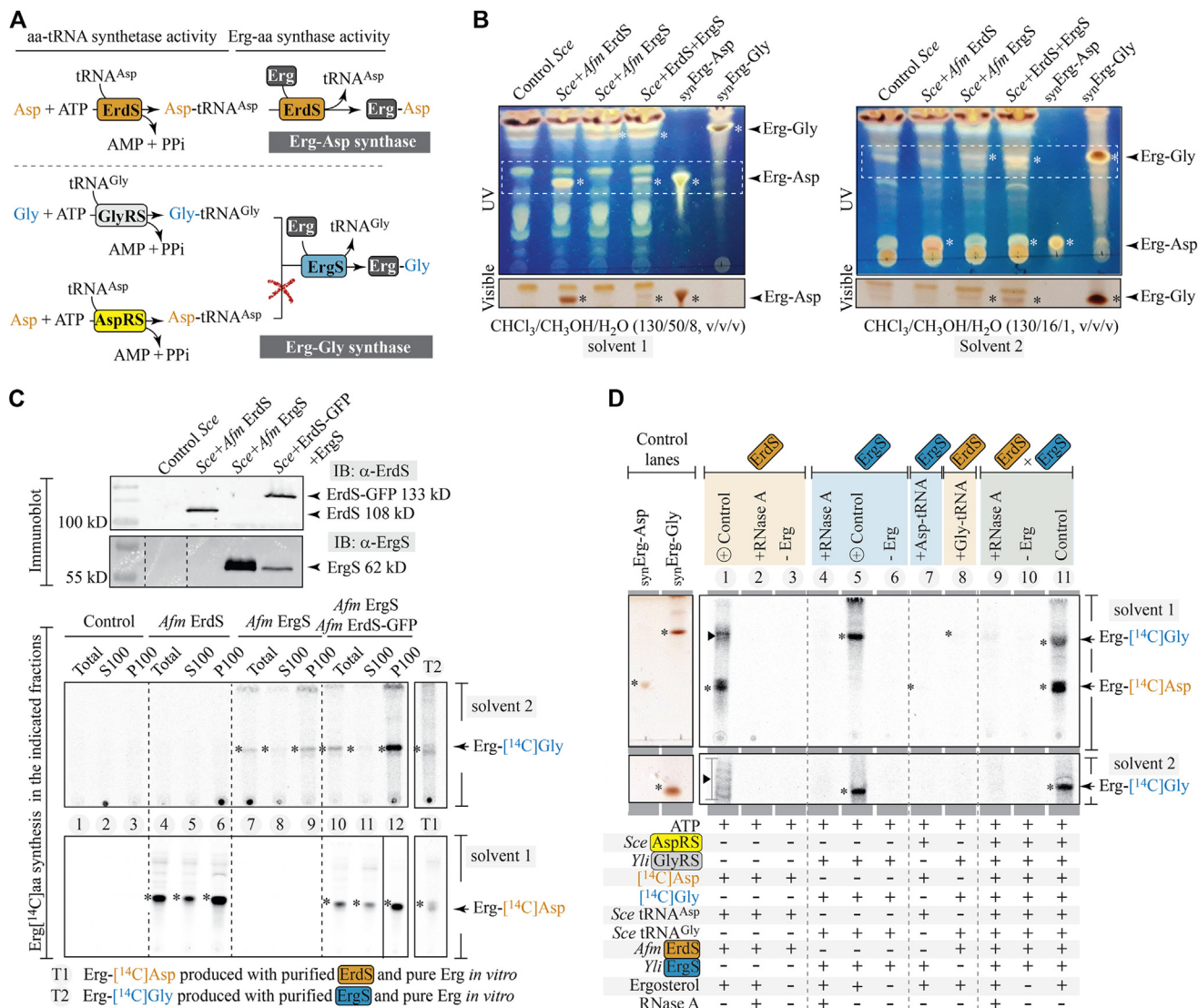
Figure 6. Specificity of ErgS and ErdS. *A*, Erg-Asp synthase (ErdS) and Erg-Gly synthase (ErgS) reaction schemes. ErgS is not expected to use Asp-tRNA^Asp produced by AspRS. *B*, TLC profiling of total lipids from *Sce* strains expressing *Afm* ErdSΔDUF (AspRS activity-only, no production of Erg-Asp), considered as the control strain, or *Afm* ErdS alone, *Afm* ErgS alone, or both *Afm* ErgS and *Afm* ErdS fused to a C-terminal Green Fluorescent Protein (GFP) tag. Migration has been conducted with two solvents as to visualize Erg-Asp and Erg-Gly simultaneously (solvent 1) or Erg-Gly alone (solvent 2). TLCs were pictured under UV light (254 nm) upon sulfuric acid/MnCl₂ staining (upper TLC) and regions delimited by *dashed boxes* are provided as visualized under white light (visible) below each panel. *Asterisks* indicate the presence of bands attributed to Erg-Asp and Erg-Gly as compared with migration profiles of synthetic (syn) Erg-Asp and Erg-Gly standards. *C*, Western blots showing expressions of *Afm* ErgS and ErdS (or ErdS-GFP) in the four tested strains (full Western blot and expression controls are provided in Fig. S8). For each of the four strains, we tested the Erg-[14C]aa synthesis activity in total proteins (total), in 100,000*g* supernatants containing soluble proteins (S100) or in the corresponding 100,000*g* pellet corresponding to total membrane-associated proteins. The upper TLC presents results obtained *in vitro* in the presence of purified *Yli* GlyRS, ATP, total tRNA, [14C]Gly to produce [14C]Gly-tRNA, to which Erg has been added (migration using solvent 1). T1 presents a control reaction under the same conditions, to which purified *Afm* ErdS was added to produce a reference Erg-[14C]Asp. The lower TLC presents results obtained *in vitro* in the presence of ATP, purified tRNA^Asp, [14C]Asp, from which ErdS produces [14C]Asp-tRNA, to which Erg has been added (migration using solvent 2). T2 presents a control reaction under the same conditions, to which purified *Yli* MBP-ErgS was added to produce a reference Erg-[14C]Gly. (Details on the composition of reactions are provided in Fig. S8.) *D*, *in vitro* Erg-[14C]aa synthesis experiments using purified *Yli* MBP-ErgS and/or *Afm* ErdS in various combinations in the presence of different combinations of tRNA and/or [14C]aa substrates. Results confirm that both enzymes are tRNA dependent and require Erg and that ErdS is specific for Asp-tRNA and ErgS for Gly-tRNA.

was distributed in both the P100 and S100 fractions, with a slight enrichment in the P100 (membrane) fraction, which was much more pronounced for ErgS activity. This was also observed in extracts from wt *Afm* (Fig. S7E). No detectable Erg-[^{14}C]Asp synthesis activity was associated with ErgS expression in the absence of ErdS, and no significant Erg-[^{14}C]Gly synthesis activity could be detected with expression of ErdS in the absence of ErgS. Only coexpression resulted in the detection of both Erg-[^{14}C]aa products (Fig. 6C, lanes 10–12), advocating for nonoverlapping specificities.

We verified the same results using purified *Afm* MBP-ErdS and *Yli*-MBP-ErgS (Fig. 6D). ErdS alone could synthesize Erg-[^{14}C]Asp from [^{14}C]Asp, ATP, and pure *Sce* tRNA^{Asp} (lane 1), whereas *Yli* ErgS produced Erg-[^{14}C]Gly in the presence of *Yli* His$_6$-GlyRS, partially fractionated *Sce* tRNA^{Gly}, [^{14}C]Gly, and ATP (lane 5). None of the enzymes functioned in the presence of RNase A (lanes 2, 4) or in the absence of Erg (lanes 3, 6). Both Erg-[^{14}C]Asp and Erg-[^{14}C]Gly were synthesized when all the required substrates and enzymes were mixed jointly with ErdS and ErgS (lane 11), unless RNase A was added (lane 9) or Erg omitted (lane 10). Lane 1 shows that ErdS produced a second product (as noted in Fig. 5C) with migration properties similar to Erg-Gly (lane 5), which could not correspond to Erg-[^{14}C]Gly, since no [^{14}C]Gly, tRNA^{Gly}, or GlyRS was present in the assay. In addition, TLC analyses using the CHCl$_3$:CH$_3$OH:H$_2$O (130:16:1, v:v:v) mobile phase (lower panel, solvent 2) showed that it contained various unidentified [^{14}C]Asp-labeled products that distributed differently from control $_{syn}$Erg-Gly and $_{syn}$Erg-Asp, or Erg-[^{14}C]Gly (lane 5), likely making these chemical species by-products of the reaction, or unspecific products resulting from the use of low-amount lipid contaminants in commercial Erg. Purified *Sce* AspRS, tRNA^{Asp}, ATP, and [^{14}C]Asp were used to produce [^{14}C]Asp-tRNA^{Asp} (lane 7) (and Fig. S7), and addition of *Yli* ErgS led to only barely detectable Erg-[^{14}C]Asp levels, showing that ErgS is highly specific toward Gly-tRNA^{Gly}. Similarly, when *Yli* His$_6$-GlyRS, fractionated tRNA^{Gly}, [^{14}C]Gly, and ATP were used to produce [^{14}C]Gly-tRNA^{Gly} (lane 8), addition of *Afm* ErdS only resulted in the synthesis of very low Erg-[^{14}C]Gly levels, showing that the transferase domain of ErdS is also highly specific for Asp-tRNA^{Asp}.

Together, these results demonstrate that the ErgS enzymes that we tested are all Gly-tRNA^{Gly}-dependent transferases that transfer Gly onto the 3β-hydroxyl of Erg, yielding Erg-Gly and that ErdS is specific for Erg-Asp production from Asp-tRNA^{Asp}. ErgS and ErdS appear to possess nonoverlapping enzymatic specificities *in vivo*.

Distribution of ErgS across Dikarya

Phylogenomics analyses show that, in contrast to ErdS, which was detected in numerous Dikarya (Ascomycota and Basidiomycota), ErgS proteins seem absent in Basidiomycota, with the exception of one species, *Trichosporon oleaginosus* (*Tol*, Fig. 1C). This suggests that ErgS is likely specific of Ascomycota. This includes most of Eurotiomycetes (*Aspergillus*, *Penicillium* spp., etc.), a large number of Sordariomycetes (*Bba*, for example), and several Dothideo- and

Leotiomycetes (Fig. 7A). Of interest, ErgS was completely absent in Saccharomycotina (10), whereas we detected one ErgS in *Yli* (Fig. 1B) and another *Yarrowia* spp. Of note, in Eurotiomycetes, Sordariomycetes, Dothideomycetes, and Leotiomycetes, when ErgS is detected, it is always found in combination with ErdS, implying that these species almost always possess both paralogs and that they likely produce Erg-Gly and Erg-Asp (Figs. 3I and 7). This is the case, for example, of all *Aspergillus* and *Penicillium* spp. studied (Eurotiomycetes). In *N. crassa* (Sordariomycetes), in which ErdS was detected and studied (10), ErgS is absent. More generally, with the exception of *Yarrowia* spp., no stand-alone ErgS was detected in all fungal species that we investigated.

Discussion

In bacteria, aaGLSs tRNA dependently modify glycerolipids (GLs) with amino acids and modulate membrane properties, increasing pathogenicity and antimicrobial resistance (17, 18). Phylogenetic analyses showed that bacterial aaGLSs are all phylogenetically related and that they can be separated into seven sequence groups (20). Most of aaPGSs possess an N-terminal transmembrane domain, in addition to the ATT/DUF2156 domain (20, 23), that is an aaGL flippase (33, 34) transferring modified lipids from the inner leaflet of the plasma membrane, where they are produced, to the outer leaflet (17, 18). No correlation has been detected between aaPGS clades and aa-tRNA and/or lipid specificities. In addition, in several bacteria, several aaGLSs coexist as paralogous enzymes and increase the diversity of modified GLs (20).

Although aaGLSs and modified GLs could be detected in numerous bacteria and several archaea, no proof on the existence of homologous eukaryotic proteins or similar amino-acylated lipids had been reported until recently (17). In Dikarya, ErdS uses L-Asp, ATP, and tRNA^{Asp} and produces Asp-tRNA^{Asp} in its so-called AspRS domain, and Asp is then transferred from its tRNA by the appended ATT/DUF2156 domain onto Erg to synthesize Erg-Asp (10) (Fig. 7B). Some bacteria possess several paralogs of aaGLSs. In Dikarya, we now demonstrated that Ascomycota possess a second, paralogous enzyme that we named ErgS and that uses the Gly-tRNA^{Gly} produced by an independent GlyRS, to form Erg-Gly (Fig. 7C). This observation shows that ergosteryl-3β-O-amino acids (Erg-aa) are diverse. ErgSs seem absent in Basidiomycota and are always found in combination with ErdS, as, for example, in all Eurotiomycetes examined, in a subset of Sordariomycetes, and in several Dothideo- and Leotiomycetes (Fig. 7A) that, like in the case of *Aor* (Fig. 3I), produce both Erg-Asp and Erg-Gly. *Yli*, which belongs to Saccharomycotina, is an exception since it only possesses ErgS and consequently only produces Erg-Gly.

The ATT (DUF2156) domain of ErgS and ErdS form two distinct phylogenetic clades (Fig. 1C). Heterologous expression of four *ergS* genes in *Sce*, as well as MS detection and characterization of Erg-Gly in *Yli* and *Aor* (Figs. 2 and 3), shows that those four ErgS proteins of interest, although scattered throughout the ErgS clade (Fig. 1C), have the same activity, which confirms that there is a good correlation between the
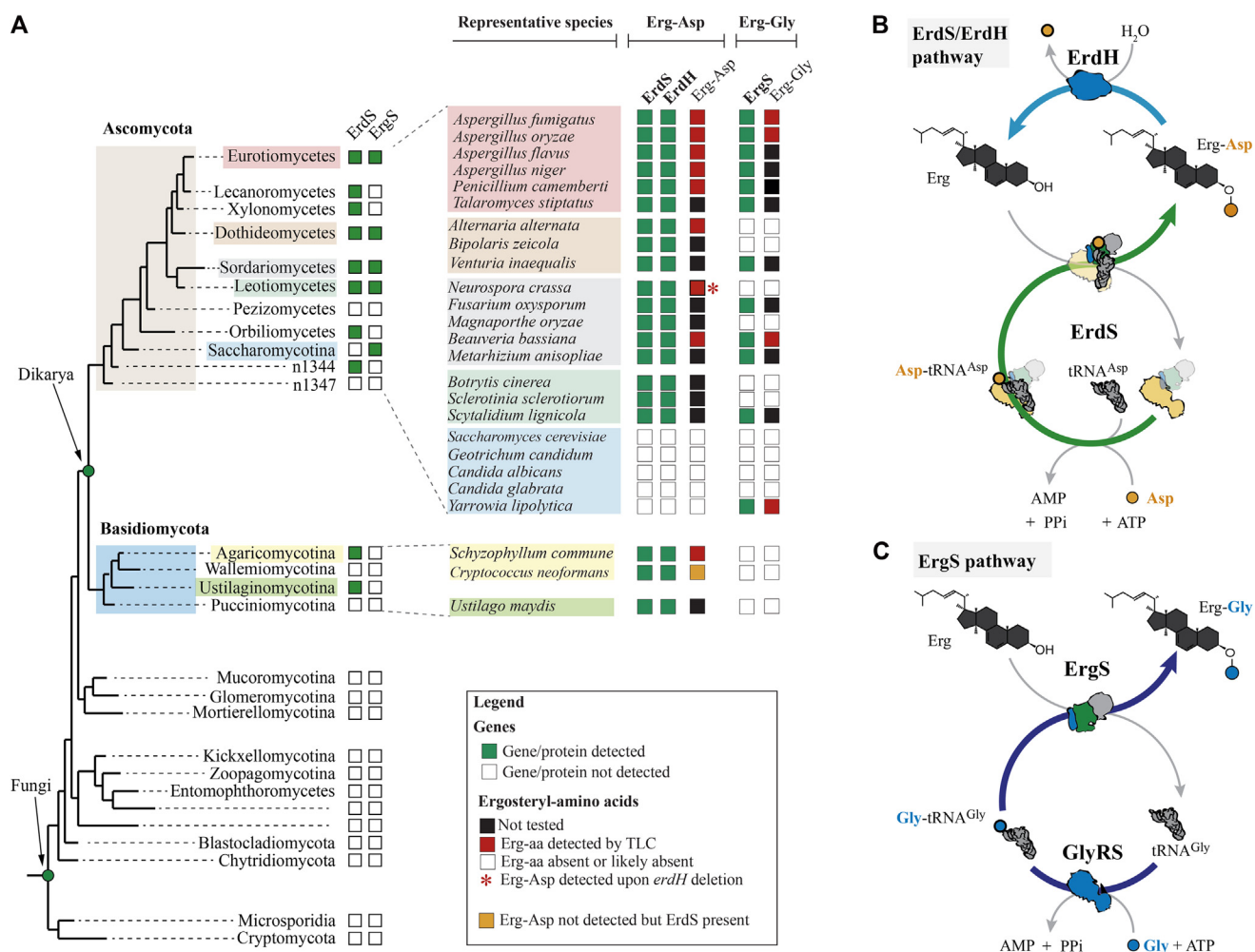
Figure 7. Distribution of ergosteryl-amino acid synthases in fungi, and overview of Erg-Gly and Erg-Asp synthesis mechanisms and factors. ErgS (Erg-Gly synthase) and ErdS (Erg-Asp synthase) sequences were searched across eukaryotes and, most specifically, in the fungal kingdom, and the presence (*green squares*) or absence (*white squares*) of the corresponding proteins was mapped onto a simplified version of the phylogenetic tree of fungi (*A*), as provided by the JGI Genome Portal (see Experimental procedures), in main fungal lineages. In Eurotiomycetes (*red*), Dothideomycetes (*light brown*), Sordariomycetes (*gray*), Leotiomycetes (*light green*), and Saccharomycotina (*blue*), the presence/absence of ErgS and ErdS was indicated in several representative species (as well as in three basidiomycetes in Agaricomycotina and Ustilaginomycotina). Erg-aa synthases are detected only in Dikarya and ErgS only in Ascomycota. *B*, Erg-Asp biosynthesis and degradation pathway. ErdS uses free L-Asp, ATP, and tRNA^{Asp} and produces Asp-tRNA^{Asp} in its AspRS domain (*yellow*), which is transferred to the appended DUF2156/ATT domain where it serves as the Asp donor for Erg-Asp synthesis. ErdH is an Erg-Asp specific hydrolase (whose distribution is indicated in (*A*)). *C*, Erg-Gly synthesis pathway. GlyRS uses Gly, ATP, and tRNA^{Gly} to produce Gly-tRNA^{Gly}, which is then released, captured by ErgS, and used as the Gly donor for Erg-Gly synthesis.

DUF2156 clade to which a fungal ATT belongs and its aa-tRNA specificity. ErdSs produce and are specific for Asp-tRNA^{Asp}, whereas ErgSs use Gly-tRNA^{Gly} (Figs. 5, 6 and S7) with no overlapping activities *in vivo*. Both enzymes amino-acylate Erg, suggesting that ErdS and ErgS may be paralogs that descended from an ancestral enzyme that already was sterol specific, *i.e.*, an Erg-aa synthase (ErxS, Er: Erg; x: amino acid in the one letter code; S: synthase). Following a putative duplication event, the two separate enzymes may have therefore undergone functional specialization for Asp-tRNA^{Asp} (ErdS) and Gly-tRNA^{Gly} (ErgS). Since ErdS is present in all Dikarya (Ascomycota and Basidiomycota), whereas ErgS only in Ascomycota, we could speculate that the duplication, if it occurred, took place only in this clade to give rise to ErgS, but this requires further and more detailed phylogenetic investigations. Both enzymes are also related to bacterial aaPGSs. Since aaPGSs are widespread in bacteria (17, 20), but

apparently absent in eukaryotes (10, 20), we can infer that ErxSs were acquired by fungi, likely through horizontal gene transfer from bacteria (35) to the last common ancestor of Dikarya. Since no known bacterial aaGLSs are sterol specific, the sterol specificity of ErxS might be a fungi-specific derived trait, but this cannot be determined at present. Precise phylogenetic analyses should therefore now be performed to (i) decipher the evolutionary history of both ErxS classes, (ii) understand the origin of their sterol and aa-tRNA specificities, (iii) determine the origin of the AspRS-DUF2156 (ErdS) fusion, and (iv) explain the asymmetric distribution of ErgS in comparison with that of ErdS. It should be emphasized that sequence identity between ErxSs and, more generally, between GNAT proteins, including DUF2156 proteins, is generally low (25). In consequence, other types of cryptic and/or highly diverged ATTs might exist in Dikarya or, alternatively, in other eukaryotes.

Erg is the main sterol lipid present within fungal membranes (9). Like Cho in mammalian cells, it influences the activity of membrane proteins, including V-ATPases that participate in antifungal drugs resistance (36, 37), participates in the formation of membrane microdomains (38, 39), and, together with sphingolipids, regulates membrane trafficking and polarized cell growth in filamentous fungi (40, 41). Even the mating process, during sexual reproduction, is dependent on the integrity of Erg for membranes fusion (42, 43) or for pheromone sensing (44). Erg also plays multiple roles in pathogenicity and antifungal resistance (9, 45, 46). In *Sce*, Erg acetylation on the 3β-hydroxyl by the Atf2 acetyltransferase and deacetylation by the Say1 esterase participates in a process that detoxifies Erg intermediates and increases resistance against membrane-disrupting agents such as the antifungal eugenol (4, 47). In addition, 3β-*O*-fatty acylation of Erg by fatty acyl-CoA transferases directs this sterol to lipid droplets where it is stored until environmental cues trigger deacylation of the fatty acid moieties by dedicated esterases for its remobilization (8, 48). Erg 3β-*O*-glycosylation by the Atg26 protein participates in the regulation of autophagy in several fungal species, including *Aspergillus* spp. (49–51), and also strongly influences virulence in pathogens (reviewed in (7)). To these physiologically important modifications of the 3β-hydroxyl of sterols, we now add aspartylation (Erg-Asp) (10) and glycylation (Erg-Gly; this study).

The biological functions of fungal Erg-aa still remain to be deciphered; however, several hypotheses can be proposed. For example, Erg-aa being modified sterols with novel chemical properties, they could be involved in sterols trafficking, like are Erg-FA (8, 48). They could also affect permeability and fluidity of fungal plasma membranes, as is the case for aminoacylated GLs in bacteria (17, 18), or in addition, could modify the properties of membrane microdomains (38). Since microdomains, enriched in Erg and sphingolipids, are crucial to the localization of drug efflux pumps (52), Erg-aa could affect drug efflux or transporters and/or membrane-localized sensing machineries that depend on Erg integrity (36, 42, 44). In other words, Erg-aa might contribute to the overall fitness of fungi under challenging environmental conditions, such as in the presence of membrane-targeting antifungals or antimicrobial peptides, as is the case for Erg-Ac in *Sce* (4, 47). In addition, Erg-Gly and Erg-Asp could directly participate in the resistance against polyenes that interact with Erg through its free 3β-OH group (53), because ErgS and ErdS add amino acids that mask this free hydroxyl group, which might change polyenes/Erg interactions and change drug susceptibility.

Lipid-derived molecules also often participate in lipid signaling in eukaryotes (41, 54), like, for example, in the case of phosphoinositides and sphingolipids (55) or sulfated sterols (3). As mentioned, Erg-Glc, another sterol conjugate, produced by Erg glycosylation, is nonessential but known to actively participate in the regulation of autophagy in several yeasts and in *Aor*, likely through the recruitment of protein partners on membrane structures (50). It is therefore possible that Erg-aa could also intervene in the recruitment of protein factors on membranes and influence regulatory or trafficking pathways.

With the discovery of a second Erg-aa synthase, we uncovered an additional subfamily of enzymes within the AATs. Further phylogenomic mining, coupled with biochemical characterization, will be needed to know whether other subfamilies of RNA-dependent sterol-aminoacylating enzymes exist. Sequence-based alignments failed to provide detailed information as to which residues of the GNAT I or GNAT II domains are responsible for lipid recognition or aa-tRNA specificity, respectively. In addition, 3D structures of ErdS and ErgS have not yet been established. Our previous work on ErdS already showed that GNAT I has a certain degree of plasticity for the recognition of the sterol substrate, since it also aspartylates Cho (10). These enzymes could therefore also aminoacylate ergosterol intermediates or derivatives having a free 3β-OH position to accept the amino acid. Likewise, it is conceivable that ErgS-like enzymes from fungal species we did not yet study might have different aa-tRNA specificities and could thus further expand the steryl-amino acid repertoire synthesized by fungi.

Experimental procedures

Reagents

All plasmids were purified using the Nucleospin Mini kit (Macherey-Nagel, 740588.50) or the NucleoBond Xtra Midi Plus kit (Macherey-Nagel, 740412.50). All enzymes for molecular cloning and Gibson Isothermal assembly were from New England Biolabs or Thermo Fisher. Thin layer chromatography (TLC, Silica gel 60 aluminum foils) plates were from Sigma-Aldrich (56524-25EA) and high-performance TLC (HPTLC) (HPTLC Silica gel 60) from Merck (1.05547.0001). Silica gel 60 for lipid purification by chromatography was from Sigma-Aldrich (Merck, ref: 227196). Commercial ergosterol was from Sigma-Aldrich (45480-10G-F), as cholesterol (C8667). All reagents and solvents were of high-grade purity. The radiolabeled amino acid mixture was from PerkinElmer (NEC850E050UC), and [^{14}C]Glycine (98 cpm/pmol, 600 μM) and [^{14}C]Asp (280 cpm/pmol) were from Amersham Life Sciences. Anti-*Afm* ErgS antibodies were developed using purified *Afm* ErgS (fDUF) with the Covalab company (France). Secondary goat anti-rabbit antibodies were from Bio-Rad (170.6516). Anti-HA antibodies were purchased from Roche (1583816) and secondary rabbit anti-mouse antibodies from Jackson Immuno Research (11035003). Synthetic Erg-Asp and synthetic Erg-Gly were prepared as described in (10, 11), respectively.

Biological resources

Strains used in this study are listed in Table S1. The *A. fumigatus* CEA17 Δ*akuB*^{KU80} (56) (kind gift from Prof. J. P. Latgé, Institute Pasteur, Paris, France) and *A. oryzae* RIB40 (57) (gift from Dr H. Nakajima) strains were used. *Y. lipolytica* (*Yli*) CLIB122 was a gift from Dr C. Bleykasten (IPCB, Strasbourg, France) and the wt *B. bassiana* 80.2 (*Bba*) strain was kindly provided by Dr D. Ferrandon (IBMC, Strasbourg, France). The *S. cerevisiae* (*Sce*) BY4742 strain (*MATα his3Δ1 leu2Δ0 lys2Δ0 ura3Δ0*) (Euroscarf) was used. The *E. coli* XL-1

Blue or DH5α strain was used as recipient strain for molecular cloning and the *E. coli* Rosetta-2 strain was used for recombinant protein expression. Primers and plasmids used in this study are reported in Table S2. For routine growth and maintenance, strains were used as indicated in the Supplementary Material and Methods section.

Total lipids extraction

Wt *Yli* and *Sce* were grown in yeast extract peptone dextrose (YPD) medium, whereas the *Sce* strains expressing *Yli*, *Afm*, *Aor*, or *Bba* ErgS were grown in Synthetic Complete media deprived of leucine (SC-Leu). Cultures were diluted to an A_{600} = 0.1 and grown overnight (220 rpm), and cells were harvested by centrifugation at 5000*g* for 15 min at 4 °C, when A_{600} was 0.6 to 1, depending on the experiment. *Aspergillus* spp. conidia were harvested as described (10) and inoculated in glass flasks (50 ml) in the YPD2 medium (Glucose 4% w/v, Peptone 1% w/v, and Yeast extract 2% w/v) at a concentration of 10^6 conidia/ml, shaken at 37 °C (*Afm*) or 30 °C (*Aor*) during 18 h. Mycelia were collected by filtration through sterile gauze and extensively washed with sterile distilled water, dried on paper towels and used for lipid extraction. *Bba* spores were collected as for *Afm*, inoculated in the YPD2 medium (50 ml) at a concentration of 10^6 spores/ml and grown for 18 h at 25 °C, and mycelia were collected by filtration through sterile gauze, washed, and dried before use.

Total lipid extraction was performed as described (10). Briefly, 50 A_{600} of *Sce* or *Yli* cells were resuspended in 0.5 ml of Na-Acetate 120 mM, pH 4.5. Then, 3.75 volumes of $CHCl_3:CH_3OH$ (2: 1) and 1 ml of glass beads (ø 0.25–0.5 mm, Roth) were added and cells were disrupted through mechanical lysis using a FastPrep Instrument (MP Biomedicals, Serial N° 10020698) at 1 min 5.5 m/s repeated 6 times. Cell lysates were incubated 3 h on a rotating wheel at 4 °C. Then, 1.25 volumes of $CHCl_3$ and 1.25 volumes of 120 mM Na-Acetate pH 4.5 were added and the samples vortexed 1 min. Phases were separated by centrifugation (9000*g*; 30 min; 4 °C), and the lower organic phase containing lipids was transferred into a clean glass tube and dried under vacuum (SpeedVac vacuum concentrator). Drying was finalized under an argon flow. Lipids were stored at –20 °C or resuspended in 50 to 100 µl of $CHCl_3:CH_3OH$ (1:1) for analysis on TLC or HPTLC. Finally, in the case of *Afm*, *Aor*, *Bba*, and other filamentous species, mechanical cell disruption was performed as described in (10). Briefly, 2 g of fresh mycelia was dried on paper towel and ground in a mortar with a pestle in the presence of liquid nitrogen and the resulting fine powder was resuspended in 1 ml (1 volume) of 120 mM Na-Acetate pH 4.5 and treated as described above.

Preparation of total, soluble, and membrane protein fractions

Sce strains carrying an empty plasmid or plasmids expressing *Afm* ErdS, *Afm* ErgS, or both enzymes were grown in liquid SC-LEU until they reached an A_{600} of 1.5. Cells were harvested by centrifugation (3000*g*, 5 min, 4 °C), washed with phosphate buffered saline (PBS), and frozen at –20 °C until use. Cells were resuspended in a solution containing 100 mM Na-Hepes buffer, pH 7.0, 30 mM KCl, 150 mM NaCl, 5 mM β-mercaptoethanol, 0.5 mM Na_2-EDTA, 1% (w/v) Triton X-100, 0.3% (w/v) NP40, 5 mM β-mercaptoethanol, and protease inhibitors tablet (Roche). One volume of glass beads (Ø 0.25–0.5 mm, Roth) was added, and cell lysis was performed with a FastPrep-24 apparatus (6 × 1 min at 6.5 m/s, with 1 min on ice between each cycle). Cell debris was removed by centrifugation at 500*g* for 10 min at 4 °C, and the supernatant centrifuged at 100,000*g* for 1 h. The resulting soluble fraction (supernatant, S100) was recovered, as well as the pellet (P100) containing total membranes and membrane-bound proteins. Membrane-bound proteins were resuspended by sonication in a solution containing 100 mM Na-Hepes buffer, pH 7.0, 30 mM KCl, 150 mM NaCl. Protein concentrations were determined using the Bradford method.

Lipid Y (Erg-Gly) purification by silica column chromatography

Total lipids were obtained from 5 g of *Yli* or *Sce* cells, with the procedure described above. Volumes were scaled up according to the initial 15 ml volume of 120 mM Na-Acetate, pH 4.5. In a glass column (1 cm × 20 cm), 8 ml of Silica Gel 60 (Sigma) was poured and washed with 4 column volumes (CV) of $CHCl_3$. Total lipids were resuspended in 500 µl of $CHCl_3$, loaded onto the column, and washed with 4 CV $CHCl_3$. Lipids were sequentially eluted using 3 CV $CHCl_3:CH_3OH$ (144:1); 3 CV $CHCl_3:CH_3OH$ (72:1), and 3 CV $CHCl_3:CH_3OH$ (36:1). Lipid fractions were dried, resuspended in 200 µl $CHCl_3:CH_3OH$ (1:1), and analyzed by TLC.

Lipid analysis by thin layer chromatography

TLC (Silica gel 60 aluminum foils, Sigma-Aldrich, 10 × 10 cm) or HPTLC (Merck, HPTLC Silica gel 60, 1.05547.0001) plates were used. Lipids in the $CHCl_3:CH_3OH$ (1:1, v:v) solvent were spotted on TLC, typically, 10 to 20 µl of total lipids or 25 µl of radiolabeled lipids extracted from *in vitro* reactions. TLCs were developed with the $CHCl_3:CH_3OH:H_2O$ mobile phase (130:50:8 or 130:16:1 (v:v:v)) for 10 min and air dried. TLCs were stained with a sulfuric acid/$MnCl_2$ solution (30) (concentrated sulfuric acid 9 ml, $MnCl_2.4H_2O$ 0.8 g, CH_3OH 120 ml, H_2O 120 ml) or with ninhydrin (Sigma-Aldrich, 0.4% w/v in EtOH 100%, v/v) and heated at 100 °C, 15 min. Plates were imaged under white light or at 254 nm. Radiolabeled lipid species were revealed by exposing TLC plates onto a Fuji Imaging Plate and analyzed with a Typhoon TRIO, Variable mode imager (GE Healthcare).

Identification of ergosteryl-3β-O-glycine by mass spectroscopy

Liquid chromatography-mass spectrometry (LC-MS) analyses of total lipid extracts were performed on a liquid chromatograph Surveyor Plus with autosampler connected to an LTQ-XL ion trap analyzer mounted with an Ion Max electrospray ionization probe (Thermo Finnigan). Lipid samples were resuspended in $CHCl_3:CH_3OH$ 2:1 and diluted 3-fold with injection solvent (isopropanol:acetonitrile:water, IPA:ACN:water, 6.5:3:0.5, v:v:v). A volume of 10 µL was injected on an Ascentis Express C18 (10 cm × 2.1 mm, 2.7 µm, Sigma-Aldrich) HPLC column at a temperature of 45 °C as described in (58) with minor

modifications. Elution was performed at a flow rate of 260 µl/min with a binary gradient where A was 60:40 water:ACN and B was 90:10 IPA:ACN. Both solutions contained 0.1% formic acid and 10 mM aqueous ammonium formate. Elution was performed with a 16-min gradient; from 0 to 1 min B was maintained at 32%, from 1 to 2.5 min B was increased to 62%, from 2.5 to 14 min to 99%, and B was maintained at 99% for 2 min. Before identification of Erg-Gly, the instrument was tuned with cholesterol in solvent B ([M-H$_2$O + H]+, m/z = 369). The LC-MS experiment shown in this article and in the supplemental section were acquired with the instrument tuned with synthetic Erg-Gly (11) in solvent B ([2M +H]+, m/z = 907). The drying gas flow rate was 20 units, and temperature of the electrospray ionization was 380 °C. Full-scan spectra were collected in the 110- to 2000-m/z range in positive mode, and data-dependent MS2 spectra were acquired on the 15 most intense MS1 peaks. MS3 spectra were acquired on the MS2 peak at m/z = 379. MS^n data were acquired with a collision-induced dissociation energy set at 35. Data were analyzed with Xcalibur Qual Browser.

Lipids extracted from wt *Aor*, wt *Sce*, and *Sce* + *Aor* fDUF were fractionated on a TSKgel ODS80tmQA (C18) column using a continuous gradient from 100% CH$_3$OH:H$_2$O (4:1, v:v) to 100% CH$_3$OH:CH$_2$Cl$_2$ (3:1, v:v). Eluted compounds were monitored at 282 nm, and peaks of interest were submitted to an Accurate-Mass Q-TOF LC-MS to confirm their identity. Synthetic Erg-Gly and Erg-Asp were used as standards to identify the same lipids.

tRNA aminoacylation reactions

Aminoacylation reactions were performed in 100 mM Na-Hepes buffer pH 7.2, containing 30 mM KCl, 12 mM MgCl$_2$, 10 mM ATP, 40 µM [^{14}C]Gly (98 cpm/pmol, Amersham Life Sciences) or 40 µM [^{14}C]Asp (280 cpm/pmol, Amersham Life Sciences), 0.1 mg/ml bovine serum albumin, 160 µM *Sce* total tRNA, 5 µM purified *Sce* tRNA^{Asp} or partially fractionated tRNA^{Gly}, and 0.05 to 0.5 µM purified *Yli*His$_6$-GlyRS or *Sce* AspRS or 6 µg of total *Sce* proteins (as a source of aaRSs) at 30 °C. Aliquots, 10 µl, were withdrawn for each time point, and [^{14}C] aa-tRNA was quantified as described (59). Pure *Sce* tRNA^{Asp} was obtained as described (10) and partially fractionated *Sce* tRNA^{Gly} was part of counter-current fractions obtained with the same procedure. *Sce* AspRS was purified as described (10).

Preparation of [^{14}C]-radiolabeled and cold Gly-tRNAs

Aminoacylation of total tRNA to prepare [^{14}C]Gly-tRNA or cold Gly-tRNA substrates for ErgS was performed essentially as described above and in (60) at 30 °C in a final volume of 100 µl in the tRNA aminoacylation mix containing 40 µM [^{14}C]Gly (98 cpm/pmol, Amersham Life Sciences) or 1 mM cold Gly and 160 µM total *Sce* tRNA. Reactions were initiated by adding 0.5 to 1.0 µM *Yli* His$_6$-GlyRS or 6 µg *Sce* total proteins, and plateaus were reached after 15 to 20 min. Reactions were then stopped by adding 0.1 vol. 3 M Na-acetate pH 4.5 (in order to preserve the ester linkage in aa-tRNAs) and 1 volume phenol. Tubes were then vortexed for 20 s, centrifuged 1 min at 10,000g at 4 °C, and the aqueous phase

was transferred to a new tube. Then, 1 volume chloroform was added, the mixture was vortexed and centrifuged 1 min at 10,000g at 4 °C, and the aqueous phase was transferred to a clean tube before adding isopropanol to a final concentration of 60% (v/v). Total aminoacylated tRNAs were precipitated at -20 °C (2 h), pelleted by centrifugation (13,000g at 4 °C), washed with 500 µl 70% ethanol, centrifuged again (13,000g at 4 °C), and the pellet was dried at room temperature for 20 min. Dried aa-tRNAs were kept at -20 °C until use. As determined with aminoacylation plateaus, total *Sce* tRNA (160 µM) contained 0.636 ± 0.014% Gly-accepting tRNAs (n = 6), *i.e.*, 1.018 ± 0.025 µM of Gly-accepting tRNA.

Lipid transfer assays

Erg and total lipids preparation

Commercial Erg was prepared in CHCl$_3$ at a concentration of 10 mg/ml. An aliquot was transferred to a clean glass tube and dried under vacuum to obtain a lipid film. Dried Erg was then resuspended by sonication (4–6 30-s pulses at maximal power, Elma S30H, Elmasonic) in a 100 mM Na-Hepes pH 7.2 buffer, supplemented with 30 mM KCl, 12 mM MgCl$_2$ to a concentration of 4 mg/ml and used immediately. Total lipids from *Sce* were prepared similarly at a final concentration of 10 mg/ml.

On-line lipid transfer assay

In order to test ErgS (Erg-Gly synthase) activity, the tRNA aminoacylation reaction was first performed as described above in a final volume of 50 µl, using 0.5 µM *Yli* His$_6$-GlyRS, 40 µM [^{14}C]Gly (98 cpm/pmol), and 160 µM total *Sce* tRNA or 5 µM fractionated *Sce* tRNA^{Gly}, to produce [^{14}C]Gly-tRNA. After 20 min, the tRNA glycylation plateau was reached (∼50–60 pmol [^{14}C]Gly-tRNA/reaction). Then Erg, suspended in a 100 mM Na-Hepes pH 7.2 buffer, supplemented with 30 mM KCl, 12 mM MgCl$_2$, was added to a final concentration of 0.5 mg/ml (total lipids to 2 mg/ml), followed by addition of purified MBP-ErgS (0.5 µM). In the case of ErdS (Erg-Asp synthase) activity, the same protocol was used with 5 µM *Sce* tRNA^{Asp} and 40 µM [^{14}C]Asp (280 cpm/pmol) to produce [^{14}C]Asp-tRNA. After 20 min, the aspartylation plateau was reached (∼50–60 pmol [^{14}C]Gly-tRNA/reaction). Erg (0.5 mg/ml) and ErdS (1 µM) were then sequentially added to initiate the transfer reaction. When protein extracts from *Sce* were used, 10 µg total proteins was added to initiate the reaction. The RNA dependency of reactions was tested in all cases using 0.3 µg RNase A incubated for 5 min in the reaction mix after the [^{14}C]aa-tRNA plateau was reached, before adding 1 µM of either ErgS or ErdS, depending on the experiment considered. To test the dependency of the presence of other substrates, these were omitted from the reaction. The mixture was then incubated 30 to 45 min at 30 °C. Reactions were stopped by adding 500 µl CHCl$_3$:CH$_3$OH:Na-Acetate (120 mM, pH 4.5) (1:2:0.8, v:v:v), vortexed for 1 min before addition of 130 µl CHCl$_3$ and 130 µl 120 mM Na-Acetate pH 4.5 to obtain a two-phase mixture. Lipids were recovered and analyzed by TLC as described above.

Isotopic competitions between free [^{14}C]Gly and cold Gly

In the case of isotopic competitions, the exact same protocol was used, using a mixture of 15 [^{14}C]aa (PerkinElmer, NEC850E050UC) in the presence of 6 µg and 160 µM total *Sce* tRNA, as to reach ∼ 50,000 cpm of [^{14}C]aa-tRNA per vial at the plateau. For isotopic competition, 5 mM cold Gly was added, before *Yli* GlyRS was used to initiate the tRNA aminoacylation reaction, in order to compete specifically with [^{14}C]Gly and [^{14}C]Gly-tRNA synthesis. Then, at the plateau, 1 µM MBP-*Yli* ErgS served to initiate the transfer reaction.

Separated LTA and competition of cold Gly-tRNA with [^{14}C]Gly-tRNA

The 50-µl reaction contained a 100 mM Na-Hepes buffer pH 7.2 supplemented with 30 mM KCl, 12 mM MgCl$_2$, and 0.5 mg/ml Erg. Dried [^{14}C]Gly-tRNAs were resuspended in water containing 1 mM MgCl$_2$ and added (200 nM per reaction) to the reaction mix. Then, 0, 100, 200, and 300 nM of purified cold Gly-tRNAs (in 1 mM MgCl$_2$) were added for isotopic competitions. The reaction was initiated by adding 1 µM MBP-ErgS. Competing cold Gly-tRNAs concentrations were evaluated knowing that Gly-accepting tRNAs represented 0.636 ± 0.014% of total tRNAs (see above). In all cases, reactions were stopped as described above.

Other methods

Strains and growth conditions for recombinant protein expression as well as purification protocols of recombinant proteins are described in Supplementary Material and Methods. Preparation of total protein extracts, conditions for Western blotting, and related protocols are described in Supplementary Material and Methods. Software, web servers, and sequences used for bioinformatical analyses are indicated in the Supplementary Material and Methods section.

Data availability

All available data are already included in the article. All materials and strains are freely available (contact: frfischer@unistra.fr; h.becker@unistra.fr; nmahmoudikaidi@unistra.fr).

References

1. Brown, M. S., and Goldstein, J. L. (1986) A receptor-mediated pathway for cholesterol homeostasis. *Science* **232**, 34–47
2. Nes, W. D. (2011) Biosynthesis of cholesterol and other sterols. *Chem. Rev.* **111**, 6423–6451
3. Mueller, J. W., Gilligan, L. C., Idkowiak, J., Arlt, W., and Foster, P. A. (2015) The regulation of steroid action by sulfation and desulfation. *Endocr. Rev.* **36**, 526–563
4. Tiwari, R., Koffel, R., and Schneiter, R. (2007) An acetylation/deacetylation cycle controls the export of sterols and steroids from S. cerevisiae. *EMBO J.* **26**, 5109–5119

5. Grille, S., Zaslawski, A., Thiele, S., Plat, J., and Warnecke, D. (2010) The functions of steryl glycosides come to those who wait: Recent advances in plants, fungi, bacteria and animals. *Prog. Lipid Res.* **49**, 262–288

6. Shimamura, M. (2020) Structure, metabolism and biological functions of steryl glycosides in mammals. *Biochem. J.* **477**, 4243–4261

7. Normile, T. G., McEvoy, K., and Del Poeta, M. (2020) Steryl glycosides in fungal pathogenesis: An understudied immunomodulatory adjuvant. *J. Fungi (Basel)* **6**, 25

8. Jacquier, N., and Schneiter, R. (2012) Mechanisms of sterol uptake and transport in yeast. *J. Steroid Biochem. Mol. Biol.* **129**, 70–78

9. Rodrigues, M. L. (2018) The multifunctional fungal ergosterol. *mBio* **9**, e01755-18

10. Yakobov, N., Fischer, F., Mahmoudi, N., Saga, Y., Grube, C. D., Roy, H., Senger, B., Grob, G., Tatematsu, S., Yokokawa, D., Mouyna, I., Latge, J. P., Nakajima, H., Kushiro, T., and Becker, H. D. (2020) RNA-dependent sterol aspartylation in fungi. *Proc. Natl. Acad. Sci. U. S. A.* **117**, 14948–14957

11. Yokokawa, D., Tatematsu, S., Takagi, R., Saga, Y., Roy, H., Fischer, F., Becker, H. D., and Kushiro, T. (2021) Synthesis of aminoacylated ergosterols: A new lipid component of fungi. *Steroids* **169**, 108823

12. Korber, M., Klein, I., and Daum, G. (2017) Steryl ester synthesis, storage and hydrolysis: A contribution to sterol homeostasis. *Biochim. Biophys. Acta Mol. Cell Biol. Lipids* **1862**, 1534–1545

13. Ruff, M., Krishnaswamy, S., Boeglin, M., Poterszman, A., Mitschler, A., Podjarny, A., Rees, B., Thierry, J. C., and Moras, D. (1991) Class II aminoacyl transfer RNA synthetases: Crystal structure of yeast aspartyl-tRNA synthetase complexed with tRNA(Asp). *Science* **252**, 1682–1689

14. Eriani, G., Cavarelli, J., Martin, F., Ador, L., Rees, B., Thierry, J. C., Gangloff, J., and Moras, D. (1995) The class II aminoacyl-tRNA synthetases and their active site: Evolutionary conservation of an ATP binding site. *J. Mol. Evol.* **40**, 499–508

15. El-Gebali, S., Mistry, J., Bateman, A., Eddy, S. R., Luciani, A., Potter, S. C., Qureshi, M., Richardson, L. J., Salazar, G. A., Smart, A., Sonnhammer, E. L. L., Hirsh, L., Paladin, L., Piovesan, D., Tosatto, S. C. E., *et al.* (2019) The Pfam protein families database in 2019. *Nucleic Acids Res.* **47**, D427–D432

16. Moutiez, M., Belin, P., and Gondry, M. (2017) Aminoacyl-tRNA-utilizing enzymes in natural product biosynthesis. *Chem. Rev.* **117**, 5578–5618

17. Fields, R. N., and Roy, H. (2018) Deciphering the tRNA-dependent lipid aminoacylation systems in bacteria: Novel components and structural advances. *RNA Biol.* **15**, 480–491

18. Slavetinsky, C., Kuhn, S., and Peschel, A. (2017) Bacterial aminoacyl phospholipids - biosynthesis and role in basic cellular processes and pathogenicity. *Biochim. Biophys. Acta Mol. Cell Biol. Lipids* **1862**, 1310–1318

19. Smith, A. M., Harrison, J. S., Sprague, K. M., and Roy, H. (2013) A conserved hydrolase responsible for the cleavage of amino-acylphosphatidylglycerol in the membrane of Enterococcus faecium. *J. Biol. Chem.* **288**, 22768–22776

20. Smith, A. M., Harrison, J. S., Grube, C. D., Sheppe, A. E., Sahara, N., Ishii, R., Nureki, O., and Roy, H. (2015) tRNA-dependent alanylation of diac-ylglycerol and phosphatidylglycerol in Corynebacterium glutamicum. *Mol. Microbiol.* **98**, 681–693

21. Arendt, W., Groenewold, M. K., Hebecker, S., Dickschat, J. S., and Moser, J. (2013) Identification and characterization of a periplasmic aminoacyl-phosphatidylglycerol hydrolase responsible for *Pseudomonas aeruginosa* lipid homeostasis. *J. Biol. Chem.* **288**, 24717–24730

22. Groenewold, M. K., Hebecker, S., Fritz, C., Czolkoss, S., Wiesselmann, M., Heinz, D. W., Jahn, D., Narberhaus, F., Aktas, M., and Moser, J. (2019) Virulence of *Agrobacterium tumefaciens* requires lipid homeostasis mediated by the lysyl-phosphatidylglycerol hydrolase AcvB. *Mol. Microbiol.* **111**, 269–286

23. Roy, H., and Ibba, M. (2008) RNA-dependent lipid remodeling by bacterial multiple peptide resistance factors. *Proc. Natl. Acad. Sci. U. S. A.* **105**, 4667–4672

24. Roy, H., and Ibba, M. (2009) Broad range amino acid specificity of RNA-dependent lipid remodeling by multiple peptide resistance factors. *J. Biol. Chem.* **284**, 29677–29683

25. Favrot, L., Blanchard, J. S., and Vergnolle, O. (2016) Bacterial GCN5-related N-acetyltransferases: From resistance to regulation. *Biochemistry* **55**, 989–1002

26. Hebecker, S., Krausze, J., Hasenkampf, T., Schneider, J., Groenewold, M., Reichelt, J., Jahn, D., Heinz, D. W., and Moser, J. (2015) Structures of two bacterial resistance factors mediating tRNA-dependent aminoacylation of phosphatidyl-glycerol with lysine or alanine. *Proc. Natl. Acad. Sci. U. S. A.* **112**, 10691–10696

27. Chang, P. K., and Ehrlich, K. C. (2010) What does genetic diversity of Aspergillus flavus tell us about Aspergillus oryzae? *Int. J. Food Microbiol.* **138**, 189–199

28. Amaike, S., and Keller, N. P. (2011) Aspergillus flavus. *Annu. Rev. Phytopathol.* **49**, 107–133

29. Lambou, K., Lamarre, C., Beau, R., Dufour, N., and Latge, J. P. (2010) Functional analysis of the superoxide dismutase family in *Aspergillus fumigatus*. *Mol. Microbiol.* **75**, 910–923

30. Goswami, S. K., and Frey, C. F. (1970) Manganous chloride spray reagent for cholesterol and bile acids on thin-layer chromatograms. *J. Chromatogr.* **53**, 389–390

31. Hemmerle, M., Wendenbaum, M., Grob, G., Yakobov, N., Mahmoudi, N., Senger, B., Debard, S., Fischer, F., and Becker, H. (2020) Noncanonical inputs and outputs of tRNA aminoacylation. *Enzymes* **48**, 117–147

32. Tsakos, M., Schaffert, E. S., Clement, L. L., Villadsen, N. L., and Poulsen, T. B. (2015) Ester coupling reactions–an enduring challenge in the chemical synthesis of bioactive natural products. *Nat. Prod. Rep.* **32**, 605–632

33. Ernst, C. M., Staubitz, P., Mishra, N. N., Yang, S. J., Hornig, G., Kalbacher, H., Bayer, A. S., Kraus, D., and Peschel, A. (2009) The bacterial defensin resistance protein MprF consists of separable domains for lipid lysinylation and antimicrobial peptide repulsion. *PLoS Pathog.* **5**, e1000660

34. Ernst, C. M., and Peschel, A. (2011) Broad-spectrum antimicrobial peptide resistance by MprF-mediated aminoacylation and flipping of phospholipids. *Mol. Microbiol.* **80**, 290–299

35. Fitzpatrick, D. A. (2012) Horizontal gene transfer in fungi. *FEMS Microbiol. Lett.* **329**, 1–8

36. Morioka, S., Shigemori, T., Hara, K., Morisaka, H., Kuroda, K., and Ueda, M. (2013) Effect of sterol composition on the activity of the yeast G-protein-coupled receptor Ste2. *Appl. Microbiol. Biotechnol.* **97**, 4013–4020

37. Zhang, Y. Q., Gamarra, S., Garcia-Effron, G., Park, S., Perlin, D. S., and Rao, R. (2010) Requirement for ergosterol in V-ATPase function underlies antifungal activity of azole drugs. *PLoS Pathog.* **6**, e1000939

38. Farnoud, A. M., Toledo, A. M., Konopka, J. B., Del Poeta, M., and London, E. (2015) Raft-like membrane domains in pathogenic microorganisms. *Curr. Top. Membr.* **75**, 233–268

39. Douglas, L. M., and Konopka, J. B. (2014) Fungal membrane organization: The eisosome concept. *Annu. Rev. Microbiol.* **68**, 377–393

40. Fischer, R., Zekert, N., and Takeshita, N. (2008) Polarized growth in fungi–interplay between the cytoskeleton, positional markers and membrane domains. *Mol. Microbiol.* **68**, 813–826

41. Rella, A., Farnoud, A. M., and Del Poeta, M. (2016) Plasma membrane lipids and their role in fungal virulence. *Prog. Lipid Res.* **61**, 63–72

42. Weichert, M., Lichius, A., Priegnitz, B. E., Brandt, U., Gottschalk, J., Nawrath, T., Groenhagen, U., Read, N. D., Schulz, S., and Fleissner, A. (2016) Accumulation of specific sterol precursors targets a MAP kinase cascade mediating cell-cell recognition and fusion. *Proc. Natl. Acad. Sci. U. S. A.* **113**, 11877–11882

43. Weichert, M., Herzog, S., Robson, S. A., Brandt, R., Priegnitz, B. E., Brandt, U., Schulz, S., and Fleissner, A. (2020) Plasma membrane fusion is specifically impacted by the molecular structure of membrane sterols during vegetative development of *Neurospora crassa*. *Genetics* **216**, 1103–1116

44. Jin, H., McCaffery, J. M., and Grote, E. (2008) Ergosterol promotes pheromone signaling and plasma membrane fusion in mating yeast. *J. Cell Biol.* **180**, 813–826

45. Alcazar-Fuoli, L., and Mellado, E. (2012) Ergosterol biosynthesis in *Aspergillus fumigatus*: Its relevance as an antifungal target and role in antifungal drug resistance. *Front. Microbiol.* **3**, 439

46. Alcazar-Fuoli, L., and Mellado, E. (2014) Current status of antifungal resistance and its impact on clinical practice. *Br. J. Haematol.* **166**, 471–484

47. Choudhary, V., Darwiche, R., Gfeller, D., Zoete, V., Michielin, O., and Schneiter, R. (2014) The caveolin-binding motif of the pathogen-related yeast protein Pry1, a member of the CAP protein superfamily, is required for *in vivo* export of cholesteryl acetate. *J. Lipid Res.* **55**, 883–894

48. Jorda, T., and Puig, S. (2020) Regulation of ergosterol biosynthesis in *Saccharomyces cerevisiae. Genes* **11**, 795

49. Nazarko, T. Y., Farre, J. C., Polupanov, A. S., Sibirny, A. A., and Subramani, S. (2007) Autophagy-related pathways and specific role of sterol glucoside in yeasts. *Autophagy* **3**, 263–265

50. Yamashita, S., Oku, M., and Sakai, Y. (2007) Functions of PI4P and sterol glucoside are necessary for the synthesis of a nascent membrane structure during pexophagy. *Autophagy* **3**, 35–37

51. Kikuma, T., Tadokoro, T., Maruyama, J. I., and Kitamoto, K. (2017) AoAtg26, a putative sterol glucosyltransferase, is required for autophagic degradation of peroxisomes, mitochondria, and nuclei in the filamentous fungus *Aspergillus oryzae. Biosci. Biotechnol. Biochem.* **81**, 384–395

52. Panwar, S. L., Pasrija, R., and Prasad, R. (2008) Membrane homoeostasis and multidrug resistance in yeast. *Biosci. Rep.* **28**, 217–228

53. Kaminski, D. M. (2014) Recent progress in the study of the interactions of amphotericin B with cholesterol and ergosterol in lipid environments. *Eur. Biophys. J.* **43**, 453–467

54. Singh, A., and Del Poeta, M. (2011) Lipid signalling in pathogenic fungi. *Cell Microbiol.* **13**, 177–185

55. De Craene, J. O., Bertazzi, D. L., Bar, S., and Friant, S. (2017) Phosphoinositides, major actors in membrane trafficking and lipid signaling pathways. *Int. J. Mol. Sci.* **18**, 634

56. da Silva Ferreira, M. E., Kress, M. R., Savoldi, M., Goldman, M. H., Hartl, A., Heinekamp, T., Brakhage, A. A., and Goldman, G. H. (2006) The akuB(KU80) mutant deficient for nonhomologous end joining is a powerful tool for analyzing pathogenicity in *Aspergillus fumigatus. Eukaryot. Cell* **5**, 207–211

57. Machida, M., Asai, K., Sano, M., Tanaka, T., Kumagai, T., Terai, G., Kusumoto, K., Arima, T., Akita, O., Kashiwagi, Y., Abe, K., Gomi, K., Horiuchi, H., Kitamoto, K., Kobayashi, T., *et al.* (2005) Genome sequencing and analysis of *Aspergillus oryzae. Nature* **438**, 1157–1161

58. Bird, S. S., Marur, V. R., Sniatynski, M. J., Greenberg, H. K., and Kristal, B. S. (2011) Serum lipidomics profiling using LC-MS and high-energy collisional dissociation fragmentation: Focus on triglyceride detection and characterization. *Anal. Chem.* **83**, 6648–6657

59. Kern, D., and Lapointe, J. (1979) The twenty aminoacyl-tRNA synthetases from *Escherichia coli*. General separation procedure, and comparison of the influence of pH and divalent cations on their catalytic activities. *Biochimie* **61**, 1257–1272

60. Bailly, M., Blaise, M., Roy, H., Deniziak, M., Lorber, B., Birck, C., Becker, H. D., and Kern, D. (2008) tRNA-dependent asparagine formation in prokaryotes: Characterization, isolation and structural and functional analysis of a ribonucleoprotein particle generating Asn-tRNA(Asn). *Methods* **44**, 146–163

61. Busso, D., Delagoutte-Busso, B., and Moras, D. (2005) Construction of a set Gateway-based destination vectors for high-throughput cloning and expression screening in Escherichia coli. *Anal. Biochem.* **343**, 313–321

62. Gibson, D. G., Young, L., Chuang, R. Y., Venter, J. C., Hutchison, C. A., 3rd, and Smith, H. O. (2009) Enzymatic assembly of DNA molecules up to several hundred kilobases. *Nat. Methods* **6**, 343–345

63. Mitchell, L. A., Cai, Y., Taylor, M., Noronha, A. M., Chuang, J., Dai, L., and Boeke, J. D. (2013) Multichange isothermal mutagenesis: a new strategy for multiple site-directed mutations in plasmid DNA. *ACS Synth. Biol.* **2**, 473–477

64. Fischer, F., Huot, J. L., Lorber, B., Diss, G., Hendrickson, T. L., Becker, H. D., Lapointe, J., and Kern, D. (2012) The asparagine-transamidosome from Helicobacter pylori: a dual-kinetic mode in non-discriminating aspartyl-tRNA synthetase safeguards the genetic code. *Nucleic Acids Res.* **40**, 4965–4976

65. Edgar, R. C. (2004) MUSCLE: a multiple sequence alignment method with reduced time and space complexity. *BMC Bioinformatics* **5**, 113

66. Kelley, L. A., Mezulis, S., Yates, C. M., Wass, M. N., and Sternberg, M. J. (2015) The Phyre2 web portal for protein modeling, prediction and analysis. *Nat. Protoc.* **10**, 845–858

67. Criscuolo, A., and Gribaldo, S. (2010) BMGE (Block Mapping and Gathering with Entropy): a new software for selection of phylogenetic informative regions from multiple sequence alignments. *BMC Evol. Biol.* **10**, 210

68. Nguyen, L. T., Schmidt, H. A., von Haeseler, A., and Minh, B. Q. (2015) IQ-TREE: a fast and effective stochastic algorithm for estimating maximum-likelihood phylogenies. *Mol. Biol. Evol.* **32**, 268–274

69. Altschul, S. F., Madden, T. L., Schaffer, A. A., Zhang, J., Zhang, Z., Miller, W., and Lipman, D. J. (1997) Gapped BLAST and PSI-BLAST: a new generation of protein database search programs. *Nucleic Acids Res.* **25**, 3389–3402

70. Grigoriev, I. V., Nikitin, R., Haridas, S., Kuo, A., Ohm, R., Otillar, R., Riley, R., Salamov, A., Zhao, X., Korzeniewski, F., Smirnova, T., Nordberg, H., Dubchak, I., and Shabalov, I. (2014) MycoCosm portal: gearing up for 1000 fungal genomes. *Nucleic Acids Res.* **42**, D699–D704

71. Kuroki, Y., Juvvadi, P. R., Arioka, M., Nakajima, H., and Kitamoto, K. (2002) Cloning and characterization of vmaA, the gene encoding a 69-kDa catalytic subunit of the vacuolar H+- ATPase during alkaline pH mediated growth of Aspergillus oryzae. *FEMS Microbiol. Lett.* **209**, 277–282

Nathaniel Yakobov has defended his PhD in 2020 at the University of Strasbourg (GMGM, UMR7156) in the team Dynamics and Plasticity of Synthetases, where he discovered the RNA-dependent ergosteryl-3β-*O*-amino acids synthesis and degradation pathways in fungi. He is currently in a post-doc position at the University of Geneva (Unige), Switzerland, in Robbie Loewith's laboratory.

Nassira Mahmoudi has a postdoc position at the University of Strasbourg (GMGM UMR7156). She has worked on infectious diseases and host–pathogens interactions. Since 2018, she has studied the ergosterol aminoacylation pathways in *Aspergillus fumigatus* in the team Dynamics and Plasticity of Synthetases. In particular, she is interested in deciphering the role of aminoacylated ergosterol in fungal physiopathology, virulence, and drug resistance.